







Zuse Institute Berlin

Takustr. 7
14195 Berlin
Germany

KAI HOPPMANN , FELIX HENNINGS , RALF LENZ ,
UWE GOTZES, NINA HEINECKE, KLAUS SPRECKELSEN,
THORSTEN KOCH 

Optimal Operation of Transient Gas Transport Networks

Zuse Institute Berlin
Takustr. 7
14195 Berlin
Germany

Telephone: +49 30-84185-0
Telefax: +49 30-84185-125

E-mail: bibliothek@zib.de
URL: <http://www.zib.de>

ZIB-Report (Print) ISSN 1438-0064
ZIB-Report (Internet) ISSN 2192-7782

Optimal Operation of Transient Gas Transport Networks

Kai Hoppmann Felix Hennings Ralf Lenz Uwe Gotzes
Nina Heinecke Klaus Spreckelsen Thorsten Koch

November 8, 2019

Abstract

In this paper we introduce a trilevel MILP formulation for the optimal operation of transient gas transport networks. Real-world gas transport networks are controlled through operating complex pipeline intersection areas, which comprise multiple compressor units, regulators, and valves. In the following, we use so-called *network stations* to model them. The technical capabilities of a station, in particular the increase of pressure through compression, are represented by purpose-built artificial arcs. Their interplay is described using the concepts of *flow directions* and co-called *simple states*. For each station and each timestep we choose a predefined flow direction, which determines where gas enters and leaves. Additionally, we choose a fitting simple state, which consists of two subsets of artificial arcs: Arcs that must and arcs that cannot be used. The objective of the overall optimization problem is to ensure that all supplies and demands are satisfied. This model was designed to make important transient global control decisions, i.e., how to route the flow and at which places to compress the gas. Afterwards, detailed technical control measures realizing them can be determined in a subsequent step. This describes the solution approach for the NAVI project conducted within the GasLab of the Research Campus MODAL, where a decision support system for dispatchers is developed.

1 Introduction

Natural gas still is and will remain one of the major energy sources in Europe [12]. Furthermore, it is often considered an important transit medium towards a low- or no-carbon future [38]. While the overall gas consumption in Germany is assumed to be constant in the future, the hourly supplies and demands at the sources and sinks of the network are expected to become more volatile. One example reason for this behaviour is the growing usage of renewable energy, e.g., solar and wind power. While their share in the energy mix is going to increase due to the planned nuclear and coal phase-outs, the production is unstable and has to be supported by natural gas fired power plants, which can be ramped-up on short notice. Hence, for the Open Grid Europe GmbH (OGE) [3], one of the largest transport system operators in Germany [2], a more robust, secure, and stable control of the network becomes inevitable in order to guarantee security of supply. Thus, the idea of a NAVI, a decision-support system for the dispatchers,

who operate the gas network, was created and realized within the GasLab of the Research Campus MODAL [1]. Given the current state of the network and a prognosis for future supplies and demands [9, 25] as well as the expected pressures at the source nodes, the goal is to determine technical control decisions realizing transport while minimizing scenario deviations and maximizing the stability of the network.

The optimization of natural gas transport through pipeline networks is a challenging task due to two crucial aspects: The physics of the gas flow and the combinatorics behind the setup of compressor units together with imposed technical restrictions and limitations. The gas flow is described by the so-called Euler equations [33], a set of non-linear hyperbolic partial differential equations (PDEs). On the other hand, compressor units can run sequentially or in parallel by opening and closing surrounding valves in order to achieve the required compression ratio and flow rate. Additionally, the compressor units feature feasible operating ranges and are subject to a non-linear power bound. More detailed explanations regarding these topics are given by Koch et al. [26].

While the stationary case, i.e., determining a feasible network state given the necessary boundary values, has gained a lot of attention in recent years, see [26] for an extensive overview, research regarding the transient case is still in the early stages. One of the first papers on transient gas transport optimization is [30]. Here, a mixed integer linear program (MILP) featuring independent single compressor units is introduced. Furthermore, the gas flow in pipelines is modelled using piecewise linear functions. Pure non-linear programs (NLPs) are considered in [28] and [39], which decide on the compression ratios of compressors, while minimizing the fuel consumption. Very recent publications are [17] and [7], both making use of special discretization schemes for the Euler equations and again considering independent single compressor units. [17] features a linear feasible region for the compressors and minimizes the deviation from the future flow and pressure values by iteratively solving a MILP and a NLP model for each timestep. In contrast, [7] imposes lower and upper bounds on the compression ratios as well as on the achievable pressure differences of the compressor units and maximizes the amount of gas stored in the network by alternatingly solving a MILP and a NLP formulation.

However, the NAVI software developed within the GasLab of the Research Campus MODAL is supposed to solve a transient gas network control problem on a large real-world network. As input, it receives the current state of the network together with future gas supplies and demands and the expected pressures at the sources. As output, highly detailed technical control recommendations, i.e., so-called *technical measures*, for all remotely controllable elements shall be given. Deviations from the given supply, demand, and pressure values, so-called *non-technical measures*, are only allowed if there exists no solution when using technical measures only. Additionally, the model has to incorporate a complete formulation of the combinatorics behind the setup of compressor stations together with an as accurate as possible physical model for the transient gas flow in pipelines. The goal is to determine a solution meeting the supplies and demands while maximizing the stability of the network. A network is considered to be stable if no control measures have to be used. Finally, due to the nature of the underlying real time application, the problem formulation has to be solvable within minutes.

Our first experiments showed that formulations satisfying all needs simultaneously were either computationally intractable or not solvable within a reasonable amount of time. Hence, we decided to split the complexity and introduced a two-stage approach. First, a transient control problem is solved using hand-tailored simplified models for the complex pipeline intersection areas, which contain all compressor stations and a majority of all other remotely controllable elements. These simplified models are called network stations and the resulting network *macroscopic*. The paper at hand deals with formulating and solving exactly this problem.

Afterwards, the resulting flow and pressure values at the boundaries of each network station are considered in a highly detailed model for the original complex pipeline intersection areas. It validates whether there exist actual technical control decisions realizing them or not [20]. Here, in a first step stationary models focusing on the combinatorics and technical restrictions of compressor stations are solved. The rationale is that the considered intersection areas contain only pipelines of short length, which cannot store or provide much gas for future usage, i.e., which do not feature a lot of *linepack*, and therefore the transient aspect can be neglected. However, the transient behaviour is included in a second step, where a corresponding mathematical model is solve using a rolling horizon approach.

In this paper, the considered transient flow problem on the macroscopic gas transport network is modelled as a trilevel program. The third level features the actual control problem and tries to maximize the stability by minimizing changes in the operation of the network stations, i.e., by minimizing the usage of technical measures. The second level minimizes the deviation from the supplies and demands necessary to guarantee feasibility for the third level. Analogously, the first level pursues the same goal but minimizes the deviation from the expected source pressures instead. In other words, the first and the second level minimize the extent of necessary non-technical measures.

Hierarchical optimization models have been used to model a variety of real world applications. Areas include but are not limited to network design [14], capacity planning [15], toll setting [6], robust unit commitment [22], or critical infrastructure protection problems [5]. More detailed overviews on possible applications can be found in [8, 23, 27]. Due to the liberalization of many energy markets, where so-called entry-exit models were introduced, new kinds of optimization problems arose in these areas. See for example [34] for a detailed description of the entry-exit model for the European natural gas market. For these new problems, hierarchical optimization turned out to be well suited for modelling purposes, not only because the entry-exit model itself can be described using a multilevel formulation [16]. For the US market for example, a discrete bilevel programming approach is used to solve a cash-out problem, where a gas shipper has to weigh daily delivery imbalances against penalties claimed by the transport company [11, 24]. For theoretical details on hierarchical and bilevel optimization we recommend [10, 29].

The remainder of this paper is structured as follows: In Section 2 we introduce the network station concept and explain how their mathematical modelling is derived. Next, in Section 3 we introduce the trilevel macroscopic transient gas flow MILP formulation, for which we present a solution approach in Section 4. We conclude with computational experiments conducted on real-world instances in Section 5 and an outlook on future improvements and extensions in Section 6.

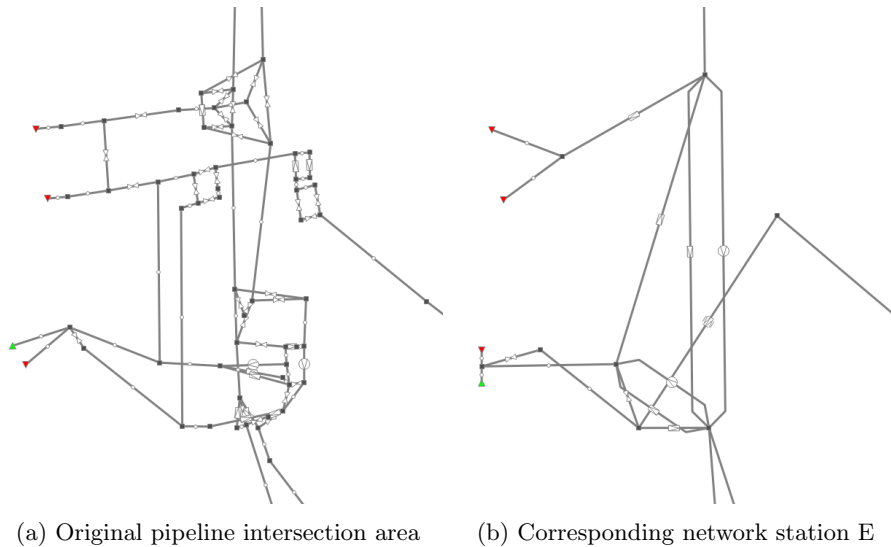


Figure 1: The colored triangles represent sources \blacktriangle and sinks \blacktriangledown , which are closely located to the network station. Further, the other single network elements are depicted as --- (pipe), $\text{---}\times\text{---}$ (valve/shortcut), $\text{---}\boxtimes\text{---}$ (regulator/regulating arc), $\text{---}\odot\text{---}$ (compressor station/compressing arc), and $\text{---}\boxplus\text{---}$ (bidirected regulating arc).

2 Network Stations

The majority of so-called *active elements* within gas networks, i.e., elements whose behaviour can be remotely controlled by the dispatchers, such as compressor stations, regulators, and valves, are located at intersections of major transportation pipelines. For each of these intersection areas and each point in time, exactly one so-called operation mode, a combination of discrete control settings for all valves and compressor stations, is in use and the settings for all other close-by active elements follow accordingly. Due to the amount of possible operation modes and the induced complexity, we developed hand-tailored simplified graph representations called network stations, which approximate the technical control capabilities, together with experts from OGE. While the detailed mathematical formulations and explanations regarding network stations can be found in Section 3.9, we briefly explain the basic idea and the process of their derivation here. An example for a simplification is depicted in Figure 1.

First, the intersection areas are identified as connected subgraphs of the network. Their layouts are created with the goal in mind to include as many active elements as possible while only containing few pipelines of significant length. The nodes at the boundaries of these subgraphs are called *fence nodes*. If a subset of the fence nodes features the same behaviour, e.g., all are connected to pipelines of large diameter, which run in parallel and nearly always possess the same pressure level as well as the same direction and amount of flow, they are merged.

Next, the interior of the subgraph is removed and *auxiliary nodes* together with so-called *artificial arcs*, which connect them and the fence nodes, are added. There are four types of artificial arcs: *Shortcuts*, which can be seen as the equivalents of valves, *regulating arcs*, which can be seen as regulators, *compressor arcs*,

which shall capture the pressure increasing capabilities of compressor stations, and *combined arcs*, which can work as either regulating or compressor arcs. Further, for each of these arc types with the exception of shortcuts there exists a bidirected version, where the gas can flow and the mentioned capabilities can be applied in both directions. Shortcuts are always bidirected by definition.

Finally, the experts from OGE looked at the possible operation modes and identified a set of so-called possible flow directions. A flow direction consists of two subsets of fence nodes: Entries, where gas enters, and exits, where gas leaves. Additionally, they developed so-called simple states. Each simple state consists of a subset of flow directions it supports and two subsets of artificial arcs: Arcs that have to be active and arcs that cannot be active. While an inactive arc can conceptually be viewed as a closed valve, active arcs have to be used according to their corresponding models, which are described in Section 3.12. The goal for the design of the simple states is to summarize and approximate the technical capabilities at the original intersection area.

3 Macroscopic Transient Gas Flow Model

In this section, we define our macroscopic transient gas flow model. We describe the entities of the underlying network and introduce variables and constraints representing their behaviour. Additionally, we explain the concepts describing their interplay and derive mathematical models for them. In the remainder of this paper, a gas network is modelled as a directed graph $G = (\mathcal{V}, \mathcal{A})$, where \mathcal{V} denotes the set of *nodes* and \mathcal{A} the set of *arcs*.

3.1 Timesteps and Granularity

Additionally, we are given a set of *timesteps* $\mathcal{T}_0 := \{0, \dots, k\}$ together with a monotonically increasing function $\tau : \mathcal{T}_0 \rightarrow \mathbb{N}$, called *granularity*. We assume that $\tau(0) = 0$. In this context, $\tau(t)$ represents the number of seconds that have passed until timestep $t \in \mathcal{T}_0$ w.r.t. timestep 0. For notational purposes we define $\mathcal{T} := \mathcal{T}_0 \setminus \{0\}$.

3.2 Boundary Values

Furthermore, $\mathcal{V}^+ \subseteq \mathcal{V}$ and $\mathcal{V}^- \subseteq \mathcal{V}$ denote the *sources* and *sinks* of the network, respectively, and we assume that $\mathcal{V}^+ \cap \mathcal{V}^- = \emptyset$. While $\mathcal{V}^b := \mathcal{V}^+ \cup \mathcal{V}^-$ is called the set of *boundary nodes*, $\mathcal{V}^0 := \mathcal{V} \setminus \mathcal{V}^b$ denotes the set of *inner nodes*.

For each boundary node $v \in \mathcal{V}^b$ and each timestep $t \in \mathcal{T}$ we are given a so-called *boundary value* $D_{v,t} \in \mathbb{R}$. They represent the future requirements in terms of supply (inflow), when $v \in \mathcal{V}^+$ is a source and we have $D_{v,t} \in \mathbb{R}_{\geq 0}$, and demand (outflow), when $v \in \mathcal{V}^-$ is a sink and we have $D_{v,t} \in \mathbb{R}_{\leq 0}$. The boundary values may be adjusted dynamically to ensure the feasibility of the model. Thus, for each boundary node $v \in \mathcal{V}^b$ and $t \in \mathcal{T}$ we introduce two continuous slack variables $\sigma_{v,t}^{d+}, \sigma_{v,t}^{d-} \in \mathbb{R}_{\geq 0}$. The actual boundary values, which are then considered in the model, are established through the additional variables $d_{v,t} \in \mathbb{R}_{\geq 0}$ for each source $v \in \mathcal{V}^+$ and $d_{v,t} \in \mathbb{R}_{\leq 0}$ for each sink $v \in \mathcal{V}^-$ and constraints

$$d_{v,t} + \sigma_{v,t}^{d+} - \sigma_{v,t}^{d-} = D_{v,t} \quad \forall v \in \mathcal{V}^b, \forall t \in \mathcal{T}. \quad (1)$$

$\sigma_{v,t}^{d+}$ and $\sigma_{v,t}^{d-}$ are called boundary value slack variables in the following. They model a set of standardized non-technical control measures, e.g., contractual options of customer interruptions and the buying or selling of so-called balancing energy.

3.3 Pressures and Pressure Bounds

Additionally, for each node $v \in \mathcal{V}$ we are given a non-negative pressure, which we denote by $p_{v,0} \in \mathbb{R}_{\geq 0}$, representing the corresponding value in the initial state. Furthermore, we introduce pressure variables $p_{v,t} \in [\underline{p}_{v,t}, \bar{p}_{v,t}] \subseteq \mathbb{R}_{\geq 0}$ for each point in time $t \in \mathcal{T}$. Here $\underline{p}_{v,t}$ is a lower and $\bar{p}_{v,t}$ is an upper bound on the pressure at node v and time t . These bounds are called *technical pressure bounds*.

For each boundary node $v \in \mathcal{V}^b$ and each point in time $t \in \mathcal{T}$ we are additionally given so-called *inflow pressure bounds* $\underline{p}_{v,t}^{\text{act}} \in \mathbb{R}_{\geq 0}$ and $\bar{p}_{v,t}^{\text{act}} \in \mathbb{R}_{\geq 0}$. These bounds are tighter than the technical pressure bounds and have to be respected if a boundary node has nonzero boundary value. They represent the expected future pressure at the sources of the network. Nevertheless, in contrast to the hard technical pressure bounds they may be relaxed using slack to ensure feasibility. Thus, we introduce two continuous variables $\sigma_{v,t}^{p+} \in [0, \underline{p}_{v,t}^{\text{act}} - \underline{p}_{v,t}]$ and $\sigma_{v,t}^{p-} \in [0, \bar{p}_{v,t} - \bar{p}_{v,t}^{\text{act}}]$ as well as constraints

$$p_{v,t} + \sigma_{v,t}^{p-} \geq \underline{p}_{v,t}^{\text{act}} \quad \forall v \in \mathcal{V}^b \text{ with } D_{v,t} \neq 0, \forall t \in \mathcal{T} \text{ and} \quad (2)$$

$$p_{v,t} - \sigma_{v,t}^{p+} \leq \bar{p}_{v,t}^{\text{act}} \quad \forall v \in \mathcal{V}^b \text{ with } D_{v,t} \neq 0, \forall t \in \mathcal{T}. \quad (3)$$

$\sigma_{v,t}^{p+}$ and $\sigma_{v,t}^{p-}$ are called inflow pressure slack variables in the following. They model the non-standardized non-technical control measure of calling neighboring transport system operators asking them to change their corresponding exit pressures in the future to a beneficial level.

3.4 Massflows

Next, we introduce variables representing the flow of gas on arcs in massflow, which we are going to call simply flow in the following. Therefore, the arc set is partitioned into four sets $\mathcal{A} = \mathcal{A}^{\text{va}} \dot{\cup} \mathcal{A}^{\text{rg}} \dot{\cup} \mathcal{A}^{\text{pi}} \dot{\cup} \mathcal{A}^{\text{ar}}$, representing the different network element we consider. Here, \mathcal{A}^{va} denotes the set of *valves*, \mathcal{A}^{rg} the set of *regulators* (often synonymously called *control valves* in the literature), \mathcal{A}^{pi} the set of *pipes*, and \mathcal{A}^{ar} the set of so-called *artificial arcs*. The artificial arcs are further partitioned into *monodirected* arcs $\mathcal{A}^{\text{ar-mo}}$ and *bidirected* arcs $\mathcal{A}^{\text{ar-bi}}$, i.e., $\mathcal{A}^{\text{ar}} = \mathcal{A}^{\text{ar-mo}} \dot{\cup} \mathcal{A}^{\text{ar-bi}}$, which is further discussed in Section 3.12. We allow parallel and anti-parallel arcs, but we do not allow loops.

For each monodirected arc $a \in \mathcal{A}^{\text{rg}} \cup \mathcal{A}^{\text{ar-mo}}$ and each timestep $t \in \mathcal{T}$ we introduce a variable $q_{a,t} \in [0, \bar{q}_{a,t}]$ representing the massflow on the corresponding arc in forward direction. On the other hand, for valves and bidirected artificial arcs we add two variables $q_{a,t}^{\rightarrow}, q_{a,t}^{\leftarrow} \in [0, \bar{q}_{a,t}]$ representing massflow in forward direction and backward direction on arc $a \in \mathcal{A}^{\text{va}} \cup \mathcal{A}^{\text{ar-bi}}$, respectively. For pipes we distinguish in- and outflow to be able to account for changes in the amount of gas which is currently stored in the pipe. Therefore, for each pipe $a = (\ell, r) \in \mathcal{A}^{\text{pi}}$ and each timestep $t \in \mathcal{T}$ we introduce two variables $q_{\ell,a,t}, q_{r,a,t} \in [-\bar{q}_{a,t}, \bar{q}_{a,t}]$ representing the massflow into a at ℓ and out of a at r . Note that negative

variable values represent massflow out of a at ℓ and into a at r , respectively. In all of the previous definitions, $\bar{q}_{a,t}$ represents a practically reasonable flow bound.

Finally, for timestep $t = 0$ and each of the variables introduced above we are given an initial massflow value, which is denoted analogously with index 0.

3.5 Massflow Conservation

Next, for all nodes $v \in \mathcal{V}$ we introduce massflow conservation equations. For each inner node $v \in \mathcal{V}^0$ and each timestep $t \in \mathcal{T}$ the amount of flow entering v has to leave it and for a boundary node $v \in \mathcal{V}^b$ supply or demand must be satisfied. Hence, we have

$$\begin{aligned} & \sum_{a=(\ell,v) \in \mathcal{A}^{va} \cup \mathcal{A}^{ar-bi}} (q_{a,t}^{\leftarrow} - q_{a,t}^{\rightarrow}) + \sum_{a=(v,r) \in \mathcal{A}^{va} \cup \mathcal{A}^{ar-bi}} (q_{a,t}^{\rightarrow} - q_{a,t}^{\leftarrow}) \\ & + \sum_{a=(v,r) \in \mathcal{A}^{rg} \cup \mathcal{A}^{ar-mo}} q_{a,t} - \sum_{a=(\ell,v) \in \mathcal{A}^{rg} \cup \mathcal{A}^{ar-mo}} q_{a,t} \\ & + \sum_{a=(v,r) \in \mathcal{A}^{pi}} q_{v,a,t} - \sum_{a=(\ell,v) \in \mathcal{A}^{pi}} q_{v,a,t} = d_{v,t} \quad \forall v \in \mathcal{V}^b, \forall t \in \mathcal{T}. \end{aligned} \quad (4)$$

For each inner node $v \in \mathcal{V}^0$ we introduce the same constraints except for the right side hand being 0.

3.6 Valves

Valves are network elements that can be used to link or unlink network parts by either creating a connection between the two corresponding endnodes or by disconnecting them. Thereby, a valve can be in one of two possible states. Either it is open, which implies that the pressure values at both ends are equal and massflow is allowed in arbitrary direction (one can think of the endnodes being merged). Or it is closed, implying that there is no massflow and the pressure values are independent or, as we synonymously call it, decoupled.

Thus, let $a = (\ell, r) \in \mathcal{A}^{va}$ be a valve in G . For each step in time $t \in \mathcal{T}$ we introduce an additional binary variable $z_{a,t} \in \{0, 1\}$ indicating whether the valve is open or not. The behaviour described above can then be modelled using the following constraints

$$p_{\ell,t} - p_{r,t} \leq (1 - z_{a,t})(\bar{p}_{\ell,t} - \underline{p}_{r,t}) \quad \forall a = (\ell, r) \in \mathcal{A}^{va}, \forall t \in \mathcal{T} \quad (5)$$

$$p_{\ell,t} - p_{r,t} \geq (1 - z_{a,t})(\underline{p}_{\ell,t} - \bar{p}_{r,t}) \quad \forall a = (\ell, r) \in \mathcal{A}^{va}, \forall t \in \mathcal{T} \quad (6)$$

$$q_{a,t}^{\rightarrow} \leq \bar{q}_{a,t} z_{a,t} \quad \forall a \in \mathcal{A}^{va}, \forall t \in \mathcal{T} \quad (7)$$

$$q_{a,t}^{\leftarrow} \leq \bar{q}_{a,t} z_{a,t} \quad \forall a \in \mathcal{A}^{va}, \forall t \in \mathcal{T}. \quad (8)$$

3.7 Regulators

Regulators can be seen as the continuous equivalent of valves. Besides being completely open or closed, regulators can also be partially open. Thereby, they generate friction due to which the gas pressure is decreased in the direction of flow. To model this behaviour, consider some $a = (\ell, r) \in \mathcal{A}^{rg}$. For each $t \in \mathcal{T}$ we add constraints

$$p_{\ell,t} - p_{r,t} \geq 0 \quad \forall t \in \mathcal{T}. \quad (9)$$

It is important to note that thereby the pressure at r can never be greater than the pressure at ℓ in our model, i.e., we do not model so-called flap traps here. This mechanism closes the regulator if a pressure at r gets greater than the pressure at ℓ and makes flow in the backward direction impossible. The reason for not including this mechanism in our model is that all regulators are considered to be connections to distribution parts of the network, i.e., parts only consisting of pipes, inner nodes and sinks, which are usually not at a higher pressure level than the upstream transportation network.

3.8 Pipes

One-dimensional gas flow in cylindric pipelines is usually described by the so-called Euler equations, a set of non-linear hyperbolic partial differential equations, together with the equation of state for real gases. In our model, for which we assume isothermality, we use the linearized formulation of Hennings [19].

Let $a = (\ell, r) \in \mathcal{A}^{\text{pi}}$ be a pipe in G . We describe the flow on a with two types of constraints, which we introduce for each timestep.

$$\begin{aligned} & \frac{2 R_s (\tau(t) - \tau(t-1)) T z_a}{L_a A_a} (q_{r,a,t} - q_{\ell,a,t}) \\ & + p_{\ell,t} - p_{\ell,t-1} + p_{r,t} - p_{r,t-1} = 0 \quad \forall t \in \mathcal{T} \end{aligned} \quad (10)$$

$$\begin{aligned} & p_{r,t} - p_{\ell,t} + \frac{\lambda_a L_a}{4 A_a D_a} (|v_{\ell,0}| q_{\ell,a,t} + |v_{r,0}| q_{r,a,t}) \\ & + \frac{g s_a L_a}{2 R_s T z_a} (p_{\ell,t} + p_{r,t}) = 0 \quad \forall t \in \mathcal{T} \end{aligned} \quad (11)$$

The parameters within these constraints are the specific gas constant R_s , the length L_a and the area of the pipe A_a , the gas temperature T , the compressibility factor z_a of the gas in the pipe, the friction factor of the pipe λ_a , the diameter D_a of the pipe, the initial absolute velocities $|v_{\ell,0}|, |v_{r,0}|$ of the gas flows at ℓ and r , the gravitational acceleration g , and the slope of the pipe $s_a = \frac{h_r - h_\ell}{L_a}$, where h_ℓ and h_r are the altitude at ℓ and r , respectively. The first constraint (10) is derived from the continuity equation of the Euler equations and captures the transient behaviour of the flow through the pipe. The second (11), derived from the momentum equation, determines the pressure loss due to friction and height difference of the endnodes.

For the friction factor we use the formula of Nikuradse [13][32]. Furthermore, we assume that the compressibility factor of the gas in the pipe is constant and determine it as the average of the compressibility factors at both endnodes using the initial pressure values and the formula of Papay [35]. Another crucial simplification to derive this linear formulation is the fixation of the absolute velocities in the friction-based pressure difference term of the momentum equation to the absolute velocities of timestep 0. If the velocity of the massflow in- or decreases significantly, we might under- or overestimate the friction loss, respectively.

3.9 Network Stations

The main idea behind the network station model and the process of how it is derived are discussed in Section 2. Formally, within G there exist $m \in \mathbb{N}$ subgraphs $G_i = (\mathcal{V}_i, \mathcal{A}_i^{\text{ar}})$ called *network stations*, which consist of inner nodes and artificial arcs only, i.e., $\mathcal{V}_i \subseteq \mathcal{V}^0$ and $\mathcal{A}_i^{\text{ar}} \subseteq \mathcal{A}^{\text{ar}}$ for all $i \in \{1, \dots, m\}$. Each artificial arc is contained in exactly one station and each inner node is contained in at most one station, i.e., $\mathcal{A}_i^{\text{ar}} \cap \mathcal{A}_j^{\text{ar}} = \emptyset$ and $\mathcal{V}_i \cap \mathcal{V}_j = \emptyset$ holds for $i, j \in \{1, \dots, m\}$ with $i \neq j$ and we have $\mathcal{A}^{\text{ar}} = \bigcup_{i=1}^m \mathcal{A}_i^{\text{ar}}$.

The node set \mathcal{V}_i can be further partitioned into so-called *fence nodes* $\mathcal{V}_i^{\text{fn}}$ and *auxiliary nodes* $\mathcal{V}_i^{\text{ar}}$, i.e., $\mathcal{V}_i := \mathcal{V}_i^{\text{fn}} \cup \mathcal{V}_i^{\text{ar}}$. A node $v \in \mathcal{V}_i$ is a fence node if it is connected to at least one arc outside the gas network station, i.e., if $\delta(v) \cap (\mathcal{A}^{\text{pi}} \cup \mathcal{A}^{\text{rg}} \cup \mathcal{A}^{\text{va}}) \neq \emptyset$, where $\delta(v)$ denotes the set of arcs incident to v . Otherwise, if $\delta(v) \subseteq \mathcal{A}_i^{\text{ar}}$, it is an auxiliary node.

Additionally, $\mathcal{F}_i \subseteq \mathcal{P}(\mathcal{V}_i^{\text{fn}}) \times \mathcal{P}(\mathcal{V}_i^{\text{fn}})$ denotes the set of so-called *flow directions* of gas network station G_i , where \mathcal{P} is the powerset operator. A flow direction $f = (f^+, f^-) \in \mathcal{F}_i$ consists of its entry fence nodes $f^+ \subseteq \mathcal{V}_i^{\text{fn}}$ and its exit fence nodes $f^- \subseteq \mathcal{V}_i^{\text{fn}}$ and it holds that $f^+ \cap f^- = \emptyset$.

Furthermore, the set $\mathcal{S}_i \subseteq \mathcal{P}(\mathcal{F}_i) \times \mathcal{P}(\mathcal{A}_i^{\text{ar}}) \times \mathcal{P}(\mathcal{A}_i^{\text{ar}})$ containing the so-called *simple states* is given for each gas network station G_i . A single simple state $s = (s^f, s^{\text{on}}, s^{\text{off}}) \in \mathcal{S}_i$ is composed of the set of flow directions s^f it supports as well as the set of its active s^{on} and its inactive artificial arcs s^{off} .

3.10 Controlling Network Stations

In each timestep $t \in \mathcal{T}_0 := \{0, \dots, k\}$ three types of control decisions have to be taken for a gas network station G_i . These decisions impact each other and can be put into a hierarchical order. Here, we describe an order in a top to bottom fashion and introduce the variables and constraints modelling the decisions and their interplay.

First of all, exactly one flow direction $f \in \mathcal{F}_i$ has to be chosen for each G_i . Given this flow direction, one must additionally choose exactly one simple state $s \in \mathcal{S}_i$ which supports this flow direction, i.e., $f \in s^f$ has to hold. Given a decision on the simple state, all arcs in s^{on} must be active, while the inactive arcs s^{off} cannot be used. For all remaining artificial arcs $a \in \mathcal{A}_i^{\text{ar}} \setminus (s^{\text{on}} \cup s^{\text{off}})$, which we call optional arcs, we independently choose whether they are active or not.

Thus, for each timestep $t \in \mathcal{T}_0$ we introduce binary variables $x_{f,t} \in \{0, 1\}$ for each flow direction $f \in \mathcal{F}_i$, $x_{s,t} \in \{0, 1\}$ for each simple state $s \in \mathcal{S}_i$, as well as $x_{a,t} \in \{0, 1\}$ for each artificial link $a \in \mathcal{A}_i^{\text{ar}}$ all indicating whether the corresponding entity is active at that point in time or not. Furthermore, for each network station G_i we add the following constraints

$$\sum_{f \in \mathcal{F}_i} x_{f,t} = 1 \quad \forall t \in \mathcal{T}_0 \quad (12)$$

$$\sum_{s \in \mathcal{S}_i} x_{s,t} = 1 \quad \forall t \in \mathcal{T}_0 \quad (13)$$

$$\sum_{f \in s^f} x_{f,t} \geq x_{s,t} \quad \forall s \in \mathcal{S}_i, \forall t \in \mathcal{T} \quad (14)$$

$$x_{s,t} \leq x_{a,t} \quad \forall s \in \mathcal{S}_i, \forall a \in s^{\text{on}}, \forall t \in \mathcal{T}_0 \quad (15)$$

$$1 - x_{s,t} \geq x_{a,t} \quad \forall s \in \mathcal{S}_i, \forall a \in s^{\text{off}}, \forall t \in \mathcal{T}_0. \quad (16)$$

While constraints (12) and (13) ensure that exactly one flow direction and one simple state are chosen for each timestep $t \in \mathcal{T}_0$, (14) guarantees that the chosen simple state supports the chosen flow direction. Additionally, constraints (15) and (16) make sure that the artificial arcs corresponding to the simple state are active or not, respectively. No condition is imposed on the optional arcs.

Next, in order to penalize changes over time w.r.t. flow directions, simple states, or artificial links in the objective function we introduce additional binary variables. For each station G_i and each timestep $t \in \mathcal{T}$ we have $\delta_{f,t} \in \{0, 1\}$ for each $f \in \mathcal{F}_i$, $\delta_{s,t} \in \{0, 1\}$ for each $s \in \mathcal{S}_i$, and $\delta_{a,t}^{\text{on}}, \delta_{a,t}^{\text{off}} \in \{0, 1\}$ for each $a \in \mathcal{A}_i^{\text{ar}}$. Furthermore, we add constraints

$$x_{f,t-1} - x_{f,t} + \delta_{f,t} \geq 0 \quad \forall f \in \mathcal{F}_i, \forall t \in \mathcal{T} \quad (17)$$

$$x_{s,t-1} - x_{s,t} + \delta_{s,t} \geq 0 \quad \forall s \in \mathcal{S}_i, \forall t \in \mathcal{T} \quad (18)$$

$$x_{a,t-1} - x_{a,t} + \delta_{a,t}^{\text{on}} - \delta_{a,t}^{\text{off}} = 0 \quad \forall a \in \mathcal{A}_i^{\text{ar}}, \forall t \in \mathcal{T}. \quad (19)$$

While $\delta_{f,t}, \delta_{s,t}, \delta_{a,t}^{\text{on}}$ indicate whether or not a flow direction, simple state, or artificial link has been switched on in timestep t , $\delta_{a,t}^{\text{off}}$ additionally indicates whether or not an artificial link has been switched off. For the flow directions and simple states we do not need such a variable, since we know that exactly one of them is active in each timestep, but in the case of optional artificial arcs this does not apply. All variables $\delta_{f,t}$ are associated with an individual cost parameter $w^f \in \mathbb{R}_{\geq 0}$, the variables $\delta_{s,t}$ with $w^s \in \mathbb{R}_{\geq 0}$, and the variables $\delta_{a,t}^{\text{on}}$ as well as $\delta_{a,t}^{\text{off}}$ are assigned a common cost parameter $w^a \in \mathbb{R}_{\geq 0}$.

3.11 Flow Direction Related Constraints

Activating a flow direction imposes certain conditions on the massflow and pressure values w.r.t. a gas network station G_i . Most importantly, for a flow direction $f = (f^+, f^-) \in \mathcal{F}_i$ no outflow is allowed at its entry and no inflow at its exit fence nodes. It is however allowed that there is no flow at all, which is the condition that must hold for all other fence nodes $v \in \mathcal{V}_i^{\text{fn}} \setminus (f^+ \cup f^-)$. Furthermore, for some of the fence nodes there exist additional pressure bounds if a flow direction is chosen in which they serve as exits. And finally, there exist conditions on the sums of absolute amounts of flow of subsets of fence nodes, which have to be satisfied in order to activate certain flow directions.

3.11.1 In- and Outflow Constraints

First of all, for each fence node $v \in \mathcal{V}_i$ and each point in time $t \in \mathcal{T}_0$ we introduce two continuous variables $q_{v,t}^{\text{in}}, q_{v,t}^{\text{out}} \in \mathbb{R}_{\geq 0}$ that, together with the following constraint, account for the total in- or outflow from outside the station, respectively

$$\begin{aligned} & \sum_{(\ell,v) \in \mathcal{A}^{\text{ar}}} q_{a,t} - \sum_{(v,r) \in \mathcal{A}^{\text{ar}}} q_{a,t} + \sum_{(\ell,v) \in \mathcal{A}^{\text{ar-bi}}} q_{a,t}^{\rightarrow} \\ - & \sum_{(\ell,v) \in \mathcal{A}^{\text{ar-bi}}} q_{a,t}^{\leftarrow} - \sum_{(v,r) \in \mathcal{A}^{\text{ar-bi}}} q_{a,t}^{\rightarrow} + \sum_{(v,r) \in \mathcal{A}^{\text{ar-bi}}} q_{a,t}^{\leftarrow} = q_{v,t}^{\text{out}} - q_{v,t}^{\text{in}}. \end{aligned} \quad (20)$$

Note that one could alternatively sum up the massflow values of the incident pipes, regulators, and valves on the left hand side and switch the signs of the variables on the right hand side of the equation. This is because flow conservation holds at the fence nodes, since $\mathcal{V}_i^{\text{fn}} \subseteq \mathcal{V}^0$. Next, for each flow direction $f = (f^+, f^-) \in \mathcal{F}_i$ we introduce the following constraints:

$$q_{v,t}^{\text{in}} \leq \bar{q}_{v,t}^{\text{in}} (1 - x_{f,t}) \quad \forall f \in \mathcal{F}_i, \forall v \in V_i \setminus f^+, \forall t \in \mathcal{T} \quad (21)$$

$$q_{v,t}^{\text{out}} \leq \bar{q}_{v,t}^{\text{out}} (1 - x_{f,t}) \quad \forall f \in \mathcal{F}_i, \forall v \in V_i \setminus f^-, \forall t \in \mathcal{T}. \quad (22)$$

Here, $\bar{q}_{v,t}^{\text{in}}$ and $\bar{q}_{v,t}^{\text{out}}$ are upper and lower bounds on the maximum possible in- and outflow, respectively, which can be derived from constraints (20) together with the above mentioned alternative constraint. If a flow direction is active, $q_{v,t}^{\text{in}}$ can be nonzero for the entry and $q_{v,t}^{\text{out}}$ for the exit fence groups only.

3.11.2 Exit Pressure Bounds

Furthermore, for some fence nodes $v \in \mathcal{V}_i^{\text{fn}}$ there exists an additional upper pressure bound \bar{p}_v^{exit} , which is tighter than its technical upper bound and has to be respected if a flow direction $f = (f^+, f^-) \in \mathcal{F}_i$ is active, for which v is an exit fence node, i.e., for which $v \in f^-$. This can be modelled via the following constraints

$$p_{v,t} \leq \bar{p}_{v,t} + x_{f,t} (\bar{p}_v^{\text{exit}} - \bar{p}_{v,t}) \quad \forall f \in \mathcal{F}_i \text{ with } v \in f^-, \forall t \in \mathcal{T}. \quad (23)$$

3.11.3 Flow Direction Conditions

Finally, for each network station, there exists a set of so-called flow direction conditions $\mathcal{W}_i \subseteq \mathcal{F}_i \times \mathcal{P}(\mathcal{V}_i^{\text{fn}}) \times \mathcal{P}(\mathcal{V}_i^{\text{fn}})$, demanding that the sum of the absolute in- and outflows of the first set of fence nodes is less than or equal than the sum of the in- and outflows of the second set in order to activate the corresponding flow direction. Hence, for each $w = (f, \mathcal{V}_{w_1}, \mathcal{V}_{w_2}) \in \mathcal{W}_i$ we introduce

$$\sum_{v \in \mathcal{V}_{w_2}} (q_{v,t}^{\text{in}} + q_{v,t}^{\text{out}}) - \sum_{v \in \mathcal{V}_{w_1}} (q_{v,t}^{\text{in}} + q_{v,t}^{\text{out}}) \geq M_{w,t} (x_{f,t} - 1) \quad \forall t \in \mathcal{T}_0 \quad (24)$$

where $M_{w,t} := \sum_{v \in \mathcal{V}_{w_1} \cap f^+} \bar{q}_{v,t}^{\text{in}} + \sum_{v \in \mathcal{V}_{w_1} \cap f^-} \bar{q}_{v,t}^{\text{out}}$. They are introduced because certain simple states with the ability to compress need these conditions in order to work.

3.12 Artificial Arcs

The set of artificial arcs can be further partitioned into four disjoint subsets $\mathcal{A}^{\text{ar}} = \mathcal{A}^{\text{ar-sc}} \cup \mathcal{A}^{\text{ar-rg}} \cup \mathcal{A}^{\text{ar-co}} \cup \mathcal{A}^{\text{ar-cb}}$. Here, $\mathcal{A}^{\text{ar-sc}}$ denotes the set of so-called *shortcuts*, $\mathcal{A}^{\text{ar-rg}}$ the set of so-called *regulating arcs*, $\mathcal{A}^{\text{ar-co}}$ the set of so-called *compressor arcs*, and $\mathcal{A}^{\text{ar-cb}}$ the set of so-called *combined arcs*. Further, we denote the set of *pressure increasing arcs* by $\mathcal{A}^{\text{ar-pr}} = \mathcal{A}^{\text{ar-co}} \cup \mathcal{A}^{\text{ar-cb}}$. The sets $\mathcal{A}_i^{\text{ar-sc}} \subseteq \mathcal{A}^{\text{ar-sc}}$, $\mathcal{A}_i^{\text{ar-rg}} \subseteq \mathcal{A}^{\text{ar-rg}}$, $\mathcal{A}_i^{\text{ar-co}} \subseteq \mathcal{A}^{\text{ar-co}}$, $\mathcal{A}_i^{\text{ar-cb}} \subseteq \mathcal{A}^{\text{ar-cb}}$, and $\mathcal{A}_i^{\text{ar-pr}} \subseteq \mathcal{A}^{\text{ar-pr}}$ describe the corresponding entities contained in gas network station G_i .

In this section we explain how the artificial arcs and their different capabilities when controlling the gas flow through the station are modelled. But first, we shortly explain the difference between bidirected and monodirected arcs.

3.12.1 Bidirected Arcs

In contrast to the monodirected arcs, massflow and pressure modifications according to the corresponding artificial arc are possible into both directions on bidirected arcs. Further, their capabilities, for example the compression of gas, are also applicable in both directions. Thus, in our model we first decide into which direction the massflow is going at each point in time.

Therefore, for each bidirected arc $a \in \mathcal{A}^{\text{ar-bi}}$ and each timestep $t \in \mathcal{T}_0$ we introduce two binary variables $x_{a,t}^{\rightarrow}, x_{a,t}^{\leftarrow} \in \{0, 1\}$ encoding the direction of the flow in case the arc is active and add constraints

$$x_{a,t}^{\rightarrow} + x_{a,t}^{\leftarrow} = x_{a,t} \quad \forall a \in \mathcal{A}^{\text{ar-bi}}, \forall t \in \mathcal{T} \quad (25)$$

to the model. Given this decision, bidirected arcs are modelled analogously to their monodirected counterparts using the corresponding variable.

3.12.2 Shortcuts

All shortcuts are bidirected arcs and massflow is possible into both directions. They can conceptually be seen as the equivalent of valves (see Section 3.6) inside a station and are used to connect network parts if the corresponding pressure levels are equal. Thus, for each shortcut $a = (\ell, r) \in \mathcal{A}^{\text{ar-sc}}$ we add constraints

$$p_{\ell,t} - p_{r,t} \leq (1 - x_{a,t})(\bar{p}_{\ell,t} - \underline{p}_{r,t}) \quad \forall t \in \mathcal{T} \quad (26)$$

$$p_{\ell,t} - p_{r,t} \geq (1 - x_{a,t})(\underline{p}_{\ell,t} - \bar{p}_{r,t}) \quad \forall t \in \mathcal{T} \quad (27)$$

$$q_{a,t}^{\rightarrow} \leq \bar{q}_{a,t} x_{a,t}^{\rightarrow} \quad \forall t \in \mathcal{T} \quad (28)$$

$$q_{a,t}^{\leftarrow} \leq \bar{q}_{a,t} x_{a,t}^{\leftarrow} \quad \forall t \in \mathcal{T}. \quad (29)$$

If a shortcut is active at time $t \in \mathcal{T}$, i.e., if $x_{a,t} = 1$, the pressures at ℓ and r have to be equal and massflow can go into an arbitrary direction with an arbitrary value, i.e., there may be forward flow $q_{a,t}^{\rightarrow} \in [0, \bar{q}_{a,t}]$ or backward flow $q_{a,t}^{\leftarrow} \in [0, \bar{q}_{a,t}]$ depending on the decision made in constraint (25). If the shortcut is not active, the pressure values are decoupled and there is no flow.

3.12.3 Regulating Arcs

Regulating arcs can conceptually be seen as the equivalent of regulators (see Section 3.7) inside a gas network station. They are used to decrease the gas

pressure in the direction of the massflow, which is needed if, for example, gas enters a distribution network, which is technically not suited for the high pressure of the transportation network. Hence, for regulating arcs $a = (\ell, r) \in \mathcal{A}^{\text{ar-rg}}$ we introduce the following constraints

$$p_{\ell,t} - p_{r,t} \geq (1 - x_{a,t})(p_{\ell,t} - \bar{p}_{r,t}) \quad \forall t \in \mathcal{T} \quad (30)$$

$$q_{a,t}^{\rightarrow} \leq \bar{q}_{a,t} x_{a,t} \quad \forall t \in \mathcal{T}. \quad (31)$$

If a regulating arc is active at some point in time $t \in \mathcal{T}$, i.e., if $x_{a,t} = 1$, the pressure at ℓ has to be greater or equal than the pressure at r . Otherwise, the pressure values are decoupled and there is no massflow. For bidirected regulating arcs $a = (\ell, r) \in \mathcal{A}^{\text{ar-rg}} \cap \mathcal{A}^{\text{ar-bi}}$, we derive an analogous set of constraints using $x_{a,t}^{\rightarrow}$ and $x_{a,t}^{\leftarrow}$ instead of $x_{a,t}$.

3.12.4 Pressure Increasing Arcs

The pressure increasing arcs $\mathcal{A}^{\text{ar-pr}}$, i.e., the compressor arcs $\mathcal{A}^{\text{ar-co}}$ and the combined arcs $\mathcal{A}^{\text{ar-cb}}$, are key elements when it comes to control a macroscopic gas network. They are able to compress gas and thereby increase its pressure, which makes up for pressure loss due to friction in the pipes or height differences that have to be overcome.

In our model, one can conceptually think of one (big) compressor unit being installed at each arc $a \in \mathcal{A}_i^{\text{ar-pr}}$ of each gas network station G_i . The maximum power it has available for compression $\tilde{\pi}_{a,t} \in \mathbb{R}_{\geq 0}$, the maximum amount of massflow that can pass through it $\tilde{q}_{a,t} \in \mathbb{R}_{\geq 0}$, and its maximum compression ratio $\tilde{r}_{a,t} \in [1, \infty)$ are dynamically determined in each timestep through an assignment of approximations of real-world compressor units, simply called *machines* in the following, and a linear combination of their corresponding values.

Thus, for each station G_i we are given a set of machines \mathcal{M}_i and each machine $m \in \mathcal{M}_i$ possesses an associated power value $P_{m,t} \in \mathbb{R}_{\geq 0}$, a maximum massflow $Q_{m,t} \in \mathbb{R}_{\geq 0}$, and a maximum compression ratio $R_{m,t} > 1$ for each timestep $t \in \mathcal{T}$. Further, for each pressure increasing arc $a \in \mathcal{A}_i^{\text{ar-pr}}$ there exists a subset of machines $\mathcal{M}_i^a \subseteq \mathcal{M}_i$ that can potentially be assigned to it and a maximum number of assignable machines M_a^{max} . Since each machine can be assigned to at most one compressing link in each timestep $t \in \mathcal{T}$, we introduce binary variables $y_{m,a,t} \in \{0, 1\}$ indicating whether machine $m \in \mathcal{M}_i$ is assigned to arc $a \in \mathcal{A}_i^{\text{ar-pr}}$ or not, and add constraints

$$\sum_{a \in \mathcal{A}_i^{\text{ar-pr}} : m \in \mathcal{M}_i^a} y_{m,a,t} \leq 1 \quad \forall m \in \mathcal{M}_i, \forall t \in \mathcal{T} \quad (32)$$

$$\sum_{m \in \mathcal{M}_i^a} y_{m,a,t} \leq M_a^{\text{max}} x_{a,t} \quad \forall a \in \mathcal{A}_i^{\text{ar-pr}}, \forall t \in \mathcal{T}. \quad (33)$$

In the real world, compressor units are operated alone, in parallel, sequentially or in a parallel-sequential setting. This is achieved by the opening and closing of valves in the surrounding piping. By setting them up in parallel, a larger amount of massflow can be compressed, while in serial a higher compression ratio can be achieved. In our model, we refrain from choosing a setup for the machines and overestimate the capabilities of pressure increasing arcs in that sense, that we assume that the maximum amount of flow (parallel setting) and the highest

compression ratio (sequential setting) are available at the same time. Thus, we add the following constraints

$$\sum_{m \in \mathcal{M}_i^a} P_{j,t} y_{m,a,t} = \tilde{\pi}_{a,t} \quad \forall a \in \mathcal{A}_i^{\text{ar-pr}}, \forall t \in \mathcal{T} \quad (34)$$

$$\sum_{m \in \mathcal{M}_i^a} Q_{j,t} y_{m,a,t} = \tilde{q}_{a,t} \quad \forall a \in \mathcal{A}_i^{\text{ar-pr}}, \forall t \in \mathcal{T} \quad (35)$$

$$1 + \sum_{m \in \mathcal{M}_i^a} (R_{j,t} - 1) y_{m,a,t} = \tilde{r}_{a,t} \quad \forall a \in \mathcal{A}_i^{\text{ar-pr}}, \forall t \in \mathcal{T}. \quad (36)$$

The first constraint (34) determines the power available on arc $a \in \mathcal{A}^{\text{ar-pr}}$ by adding up the maximum power of the assigned machines. Analogously, the second constraint (35) determines the maximum amount of massflow that can be compressed. On the other hand, the third constraint (36) is a (conservative) approximation of the maximum compression ratio, which is used in order to avoid non-linear constraints.

Finally, the connection between pressure difference, the amount of massflow passing through a compressor machine, and the power necessary to realize it is given by the non-linear *power equation* for compressor machines

$$\tilde{\pi}_{a,t} \geq \pi_{a,t} = \frac{q_{a,t}}{\eta_{\text{ad}}} R_s T z_l \frac{\kappa}{\kappa - 1} \left[\left(\frac{p_{r,t}}{p_{\ell,t}} \right)^{\frac{\kappa-1}{\kappa}} - 1 \right],$$

where $\pi_{a,t} \in \mathbb{R}_{\geq 0}$ is the variable representing the necessary power when a massflow of $q_{a,t}$ with initial pressure $p_{\ell,t}$ shall be compressed up to $p_{r,t}$. Here, η_{ad} is the adiabatic efficiency of the compression, which we assume to be constant for all existing compressor machines, and $\kappa = 1.296$ [13].

To avoid introducing this non-linear constraint we determine a linear approximation as follows. For each artificial compressing link $a \in \mathcal{A}^{\text{ar-pr}}$ and each $t \in \mathcal{T}$, we sample N points $(p_{\ell,t}, p_{r,t}, \pi_{a,t}) \in [p_{\ell,t}, \bar{p}_{\ell,t}] \times [p_{r,t}, \bar{p}_{r,t}] \times [\frac{\pi_{a,t}^{\text{max}}}{4}, \pi_{a,t}^{\text{max}}]$, where $\pi_{a,t}^{\text{max}}$ is the maximum possible power for a at t derived from (32) and (33), such that $p_{\ell,t} \leq p_{r,t}$ and determine the corresponding massflow $q_{a,t}$ using the original power equation. To the resulting set of 4-tuples we apply an ordinary least-squares method and determine coefficients $(\alpha_0, \alpha_1, \alpha_2, \alpha_3)$ for a linear approximation, which gives rise to constraints

$$\alpha_0 + \alpha_1 p_{\ell,t} + \alpha_2 p_{r,t} + \alpha_3 q_{a,t} \leq \pi_{a,t} + (1 - x_{a,t})(\alpha_0 + \alpha_1 \bar{p}_{\ell,t} + \alpha_2 \bar{p}_{r,t}), \quad (37)$$

$$\alpha_0 + \alpha_1 p_{\ell,t} + \alpha_2 p_{r,t} + \alpha_3 q_{a,t} \geq \pi_{a,t} + (1 - x_{a,t})(\alpha_0 + \alpha_1 \bar{p}_{\ell,t} + \alpha_2 \bar{p}_{r,t}), \quad (38)$$

where we assume that $\alpha_1 \in \mathbb{R}_{\leq 0}$ and $\alpha_2 \in \mathbb{R}_{\geq 0}$ (otherwise we use the corresponding other bound for the coefficients of $x_{a,t}$ on the right hand sides). If the pressure increasing arc is active, it has to respect this linear approximation. Otherwise, there is no flow and the pressures at both ends are decoupled. Finally, we add the following set of constraints

$$\pi_{a,t} \leq \tilde{\pi}_{a,t} \quad \forall a \in \mathcal{A}_i^{\text{ar-pr}}, \forall t \in \mathcal{T} \quad (39)$$

$$q_{a,t} \leq \tilde{q}_{a,t} \quad \forall a \in \mathcal{A}_i^{\text{ar-pr}}, \forall t \in \mathcal{T} \quad (40)$$

$$p_{\ell,0} \tilde{r}_{a,t} - p_{r,t} \geq (1 - x_{a,t})(p_{\ell,0} - \bar{p}_{r,t}) \quad \forall a \in \mathcal{A}_i^{\text{ar-pr}}, \forall t \in \mathcal{T}. \quad (41)$$

The first two constraints (39) and (40) ensure that the massflow and power used for compression do not violate the upper bounds given by the machine assignments. Finally, the outgoing pressure is bounded by the product of the initial ingoing pressure at $t = 0$ and the current maximum compression ratio (41) if the corresponding arc is active. Using the pressure variables instead would again result in non-linear constraints.

3.12.5 Compressor Arcs

Besides constraints (32) – (41), for each compressor arc $a = (\ell, r) \in \mathcal{A}^{\text{ar-co}}$ and each timestep $t \in \mathcal{T}$ we add constraints

$$p_{\ell,t} - p_{r,t} \leq (1 - x_{a,t})(\bar{p}_{\ell,t} - \underline{p}_{r,t}) \quad \forall t \in \mathcal{T} \quad (42)$$

$$r_{a,t}^{\max} p_{\ell,t} - p_{r,t} \geq (1 - x_{a,t})(r_{a,t}^{\max} \underline{p}_{\ell,t} - \bar{p}_{r,t}) \quad \forall t \in \mathcal{T}. \quad (43)$$

If the arc is active at some point in time $t \in \mathcal{T}$, i.e., $x_{a,t} = 1$, the pressure at ℓ has to be smaller than or equal to the pressure at r . Further, we bound $p_{r,t}$ by $r_{a,t}^{\max} p_{\ell,t}$ where $r_{a,t}^{\max}$ is the maximum possible compression ratio of a at time t , which can be derived from constraints (33) and (41). If it is not active, the pressure values are decoupled and there is no massflow due to constraints (40) and (35).

Further, there may be an additional upper bound on the pressure at node r , which has to be respected if the arc is active. Let $\bar{p}_{r,t}^{\text{out}}$ denote this upper bound. We can model this requirement by:

$$p_{r,t} \leq \bar{p}_{r,t} - x_{a,t}(\bar{p}_{r,t} - \bar{p}_{r,t}^{\text{out}}) \quad \forall t \in \mathcal{T}. \quad (44)$$

If such a bound is given, we shrink the sample space described in the previous section, accordingly.

3.12.6 Combined Arcs

A combined arc $a = (\ell, r) \in \mathcal{A}_i^{\text{ar-cb}}$ can be used as a regulating or a compressor arc. Hence, we first of all introduce two binary decision variables encoding in which mode it is activated.

$$x_{a,t}^{\text{rg}} + x_{a,t}^{\text{cp}} = x_{a,t} \quad \forall a \in \mathcal{A}_i^{\text{ar-cb}}, \forall t \in \mathcal{T} \quad (45)$$

All constraints (32) – (41), where $x_{a,t}$ is replaced by $x_{a,t}^{\text{cp}}$ in (33), (37), (38), and (41), are added for each combined arcs except for (40), which is replaced by

$$q_{a,t} \leq \tilde{q}_{a,t} + \bar{q}_{a,t} x_{a,t}^{\text{rg}} \quad \forall a \in \mathcal{A}_i^{\text{ar-cb}}, \forall t \in \mathcal{T}, \quad (46)$$

since $\tilde{q}_{a,t} = 0$ holds if $x_{a,t}^{\text{rg}} = 1$. To capture the behaviour as regulating arc, we add constraints

$$p_{\ell,t} - p_{r,t} \geq (1 - x_{a,t}^{\text{rg}})(\underline{p}_{\ell,t} - \bar{p}_{r,t}) \quad \forall t \in \mathcal{T} \quad (47)$$

analogously to (9), while for the pressure increasing arc we additionally have

$$p_{\ell,t} - p_{r,t} \leq (1 - x_{a,t}^{\text{cp}})(\bar{p}_{\ell,t} - \underline{p}_{r,t}) \quad \forall t \in \mathcal{T} \quad (48)$$

$$r_{a,t}^{\max} p_{\ell,t} - p_{r,t} \geq (1 - x_{a,t}^{\text{cp}})(r_{a,t}^{\max} \underline{p}_{\ell,t} - \bar{p}_{r,t}) \quad \forall t \in \mathcal{T}, \quad (49)$$

analogously to (42) and (43). Further, as for the compressor arcs, there may be an additional upper bound on the pressure at node r , if compression is used. Thus, we add

$$p_{r,t} \leq \bar{p}_{r,t} - x_{a,t}^{\text{cp}}(\bar{p}_{r,t} - \bar{p}_{r,t}^{\text{out}}) \quad \forall t \in \mathcal{T}, \quad (50)$$

similar to (44), and also shrink the sample space from the previous section, accordingly.

3.13 Objectives

As mentioned in the introduction, we solve a hierarchical MILP formulation consisting of three levels, i.e., a trilevel mixed-integer linear program. This is motivated by the following rationale. In the real-world dispatchers first of all try to control the network by using technical measures only, i.e., by using and changing the setting of the active elements in order to satisfy the supplies and demands desired by the customers. If this does not seem to work, they have standardized some non-technical measures at hand. The most common ones are the change of supplies and demands by either by buying or selling gas, i.e., using so-called balancing energy, or by using contractual options like the interruption of customers. If changing the supplies and demands alone does not work out, the last option is to ask other transport system operator for pressure changes of the future supply at some source nodes. In practice, this is done by phone calls and can therefore be seen as the last possible non-standardized option.

Thus, the complete trilevel MILP formulation can be stated as

$$\min_{\sigma^p} \sum_{t \in \mathcal{T}} \sum_{v \in \mathcal{V}^b} (\sigma_{v,t}^{p+} + \sigma_{v,t}^{p-}) \quad (51)$$

$$\min_{\sigma^d} \sum_{t \in \mathcal{T}} \sum_{v \in \mathcal{V}^b} (\sigma_{v,t}^{d+} + \sigma_{v,t}^{d-}) \quad (52)$$

$$\min_{\delta} \sum_{t \in \mathcal{T}} \left(\sum_{f \in \mathcal{F}} w^f \delta_{f,t} + \sum_{s \in \mathcal{S}} w^s \delta_{s,t} + \sum_{a \in \mathcal{A}^{\text{ar}}} w^a (\delta_{a,t}^{\text{on}} + \delta_{a,t}^{\text{off}}) \right) \quad (53)$$

$$\text{s.t. (1) - (50)}$$

In our model the first level controls the slack variables for the inflow pressure bounds, while the second level controls the slack variables for the boundary values. The goal of both levels is to minimize the sum of the corresponding slack variables. The third level, which can be seen as the level actually controlling the network while the other two only ensure feasibility, controls the remaining variables and minimizes the total cost, which is given as the weighted sum of flow direction, simple state and auxiliary link changes.

4 Algorithmic Framework

To formally define the algorithmic framework for solving the trilevel MILP model, we define three closely connected (single level) MILP models: First, the MILP consisting of objective function (53) and constraint set (1)–(50) with all slack variables being fixed to zero we call L3. Second, objective function (52) together with (1)–(50) as well as all inflow pressure slack variables being fixed to zero we denote by L2. And third, (51) combined with (1)–(50) describes MILP formulation L1, which is often called high point relaxation in the context of hierarchical optimization. The algorithmic framework is stated in Algorithm 1.

Input : Trilevel MILP
Output: An optimal solution or INFEASIBLE

```

1 Solve L3
2 if L3 is infeasible then
3   Solve L2
4   if L2 is infeasible then
5     Solve L1
6     if L1 is infeasible then
7       return INFEASIBLE
8     else
9       SOL1 ← Optimal solution for L1
10       $\tilde{L}_2 \leftarrow L_2$  but inflow pressure slacks fixed to SOL1
11      Solve  $\tilde{L}_2$ 
12       $\tilde{SOL}_2 \leftarrow$  Optimal solution for  $\tilde{L}_2$ 
13       $\tilde{L}_3 \leftarrow L_3$  but both slack types fixed to  $\tilde{SOL}_2$ 
14      Solve  $\tilde{L}_3$ 
15      return Optimal solution for  $\tilde{L}_3$ 
16    else
17      SOL2 ← Optimal solution for L2
18       $\hat{L}_3 \leftarrow L_3$  but both slack types fixed to SOL2
19      return Optimal solution for  $\hat{L}_3$ 
20  else
21  return Optimal solution for L3

```

Algorithm 1: Algorithmic Framework

If there exists a feasible solution with no slacks, i.e., for L₃, an optimal solution is returned as an optimal solution for the trilevel MILP in line (21). Otherwise, if there exists a feasible solution for L₂, we subsequently solve \hat{L}_3 , i.e., L₃ with the all slack variables fixed to an optimal solution of L₂. Doing this, we determine an optimal solution for the overall trilevel program, see lines (17)–(19). Finally, if L₂ does not admit a feasible solution, we consider the high point relaxation L₁. If it is infeasible, the whole problem is infeasible (7). Otherwise, we subsequently solve \tilde{L}_2 and \tilde{L}_3 to determine an overall optimal solution, see lines (9)–(15).

4.1 Heuristics for MILP Formulations

Next, we introduce two heuristics that can be applied to the MILP models from the previous section, i.e., to $L_1, L_2, \tilde{L}_2, L_3, \tilde{L}_3$, or \hat{L}_3 .

First, we introduce a rolling horizon approach. We start by solving the model for variables and constraints corresponding to $t = 0$ only. Then, in each of the following n iterations we solve the model where the next timestep is added and the binary decisions of all but the newly added timestep are fixed to the solution values from the previous iteration.

The second heuristic initially solves a specially designed Min-Cost-Flow (MCF) problem defined on $G = (\mathcal{V}, \mathcal{A})$ for each timestep $t \in \mathcal{T}$. Analyzing the in- and outflows at the fence nodes of each station in the optimal solutions, we reduce the number of possible flow directions by fixing binary variables of those flow directions for this timestep to zero, which are not consistent with the MCF solution.

4.1.1 Rolling Horizon Heuristic

The first idea to determine a feasible solution for any of the MILP models is to use a rolling horizon approach, i.e., to iteratively consider the model with an additional timestep, solve it, and fix the binary decision variables of the next iteration to the values of the corresponding binary variables of an optimal solution of the current iteration. The procedure is described in Algorithm 2.

If any of the models MIP_k is infeasible, we stop the heuristic and return UNSUCCESSFUL. Otherwise, the heuristic terminates with a feasible solution. Rolling horizon style approaches have been widely used to find feasible solutions for time-dependent optimization problems, for example for disruption management in the railway industry [31] or for scheduling problems [4][36].

```

Input : MILP model  $L_1, L_2, \tilde{L}_2, L_3, \tilde{L}_3$ , or  $\hat{L}_3$ 
Output: Feasible solution  $SOL_n$  or UNSUCCESSFUL
1 for  $k \leftarrow 0$  to  $n$  do
2    $MIP_k \leftarrow$  model for  $\mathcal{T}_0 := \{0, \dots, k\}$ 
3   for  $i \leftarrow 0$  to  $k - 1$  do
4     | Fix binary variables for timestep  $i$  in  $MIP_k$  to  $SOL_{k-1}$ 
5     Solve  $MIP_k$ 
6     if  $MIP_k$  is infeasible then
7       | return UNSUCCESSFUL
8     else
9       |  $SOL_k \leftarrow$  Optimal solution for  $MIP_k$ 
10 return  $SOL_n$ 

```

Algorithm 2: Rolling Horizon Heuristic (RHH)

4.1.2 A Min-Cost-Flow Based Heuristic

The idea behind the MCF heuristic is to decrease the number of binary variables regarding the flow directions in the MILP formulation by fixing a subset of them for each timestep to zero. Due to the hierarchical structure of the decisions in a station, further fixations, for example for binary variables corresponding to simple states, may follow. In order to exclude certain flow directions, we solve a specially

designed MCF problem on the underlying graph for each timestep and analyze the in- and outflows at the fence nodes. Besides the existence of fast algorithms for solving it, MCF is often used in practice by transport system operators to approximate the flow of natural gas, see for example [21][37], where it is used to determine worst case transport scenarios.

For each arc $a \in \mathcal{A}^{\text{rg}} \cup \mathcal{A}^{\text{ar-mo}}$ we introduce a non-negative flow variable $f_a \in \mathbb{R}_{\geq 0}$ and for each $a \in \mathcal{A}^{\text{va}} \cup \mathcal{A}^{\text{pi}} \cup \mathcal{A}^{\text{ar-bi}}$ we introduce two non-negative flow variables $f_a^{\rightarrow}, f_a^{\leftarrow} \in \mathbb{R}_{\geq 0}$ describing the forward and the backward flow, respectively. Further, consider some $t \in \mathcal{T}$ and w.l.o.g. we have $\sum_{v \in \mathcal{V}^+} D_{v,t} \geq \sum_{v \in \mathcal{V}^-} |D_{v,t}| > 0$ and let $\chi_t := \frac{\sum_{v \in \mathcal{V}^+} D_{v,t}}{\sum_{v \in \mathcal{V}^-} |D_{v,t}|}$. Additionally, recall that for each pipe $a \in \mathcal{A}$ we are given its length $\ell_a \in \mathbb{R}_{\geq 0}$. Finally, the MCF we solve for each timestep t can be formulated as the following linear program (LP)

$$\min \sum_{a \in \mathcal{A}^{\text{pi}}} L_a(f_a^{\rightarrow} + f_a^{\leftarrow}) \quad (54)$$

$$\begin{aligned} & \sum_{(v,r) \in \mathcal{A}^{\text{rg}} \cup \mathcal{A}^{\text{ar-mo}}} f_a + \sum_{(v,r) \in \mathcal{A}^{\text{va}} \cup \mathcal{A}^{\text{pi}} \cup \mathcal{A}^{\text{ar-bi}}} (f_a^{\rightarrow} - f_a^{\leftarrow}) \\ - & \sum_{(\ell,v) \in \mathcal{A}^{\text{rg}} \cup \mathcal{A}^{\text{ar-mo}}} f_a + \sum_{(\ell,v) \in \mathcal{A}^{\text{va}} \cup \mathcal{A}^{\text{pi}} \cup \mathcal{A}^{\text{ar-bi}}} (f_a^{\leftarrow} - f_a^{\rightarrow}) = 0 \quad \forall v \in \mathcal{V}^0 \end{aligned} \quad (55)$$

$$\begin{aligned} & \sum_{(v,r) \in \mathcal{A}^{\text{rg}} \cup \mathcal{A}^{\text{ar-mo}}} f_a + \sum_{(v,r) \in \mathcal{A}^{\text{va}} \cup \mathcal{A}^{\text{pi}} \cup \mathcal{A}^{\text{ar-bi}}} (f_a^{\rightarrow} - f_a^{\leftarrow}) \\ - & \sum_{(\ell,v) \in \mathcal{A}^{\text{rg}} \cup \mathcal{A}^{\text{ar-mo}}} f_a + \sum_{(\ell,v) \in \mathcal{A}^{\text{va}} \cup \mathcal{A}^{\text{pi}} \cup \mathcal{A}^{\text{ar-bi}}} (f_a^{\leftarrow} - f_a^{\rightarrow}) = D_{v,t} \quad \forall v \in \mathcal{V}^+ \end{aligned} \quad (56)$$

$$\begin{aligned} & \sum_{(v,r) \in \mathcal{A}^{\text{rg}} \cup \mathcal{A}^{\text{ar-mo}}} f_a + \sum_{(v,r) \in \mathcal{A}^{\text{va}} \cup \mathcal{A}^{\text{pi}} \cup \mathcal{A}^{\text{ar-bi}}} (f_a^{\rightarrow} - f_a^{\leftarrow}) \\ - & \sum_{(\ell,v) \in \mathcal{A}^{\text{rg}} \cup \mathcal{A}^{\text{ar-mo}}} f_a + \sum_{(\ell,v) \in \mathcal{A}^{\text{va}} \cup \mathcal{A}^{\text{pi}} \cup \mathcal{A}^{\text{ar-bi}}} (f_a^{\leftarrow} - f_a^{\rightarrow}) = \chi_t D_{v,t} \quad \forall v \in \mathcal{V}^-. \end{aligned} \quad (57)$$

Note that if there is no supply or demand in a timestep, we define the right hand sides of all constraints to be 0. Now, given an optimal solution, for each gas network station G_i and each of its fence nodes $v \in \mathcal{V}_i^{\text{fn}}$ we check whether there is in- or outflow w.r.t. to G_i at v . If for

$$f_v := \sum_{(v,r) \in \mathcal{A}^{\text{ar-mo}}} f_a + \sum_{(v,r) \in \mathcal{A}^{\text{ar-bi}}} (f_a^{\rightarrow} - f_a^{\leftarrow}) - \sum_{(\ell,v) \in \mathcal{A}^{\text{ar-mo}}} f_a + \sum_{(\ell,v) \in \mathcal{A}^{\text{ar-bi}}} (f_a^{\leftarrow} - f_a^{\rightarrow})$$

we have $f_v \in \mathbb{R}_{\geq 0} \setminus [0, \varepsilon)$ we call v a MCF entry fence node and if $f_v \in \mathbb{R}_{\leq 0} \setminus (\varepsilon, 0]$ we call it an MCF exit fence node. The idea to use some $\varepsilon \in \mathbb{R}_{\geq 0}$ in this definition is that small in- and outflows could be realized by using the gas stored in adjacent pipelines, i.e., linepack.

Next, we call a flow direction $f = (f^+, f^-)$ MCF-valid for station G_i and timestep t , if for each MCF entry fence node v we have $v \in f^+$ and for each MCF exit fence node v we have $v \in f^-$. As the final step of the heuristic, we solve the MIP model as described in Section 3, where we fix for each station G_i and each timestep $t \in \mathcal{T}$ all binary variables corresponding to flow directions which are not MCF-valid to zero, if there exists at least one MCF-valid flow direction. Otherwise, we do not apply any fixations.

5 Computational Results

In this section we present computational experiments, which were conducted in order to check whether the presented model is suitable to make important transient global control decisions in the first stage of the NAVI algorithm or not. First, we describe the set of our test instances, followed by the computational setup. We conclude the section with an analysis of the obtained results.

$ \mathcal{V} $	$ \mathcal{V}^+ $	$ \mathcal{V}^- $	$ \mathcal{A}^{\text{pi}} $	$ \mathcal{A}^{\text{rg}} $	$ \mathcal{A}^{\text{va}} $	$ \mathcal{A}^{\text{ar}} $
179	12	89	149	5	1	67

Table 1: Composition of the macroscopic gas network.

5.1 Instances

For our computations we used 333 instances provided by our project partner OGE, which are based on a real-world network and the corresponding historically measured data. Thus, the initial state, the boundary values, and the source pressures represent feasible network states. Non-technical control decisions, which were undertaken by the dispatchers during the considered time horizon, are already included in this data. Hence, if the model would perfectly capture reality, we expect it to find feasible solutions without using slack.

While the overall composition of the network is depicted in Table 1, the properties of the 7 network stations, which it features, are shown in Table 2. In the following, we considered two different datasets. Dataset 1 consists of 168 instances in 30 minute intervals starting at noon of a virtual day 1 and ending of 23:30pm of virtual day 4. The other set consists of 165 instances starting at midnight of a virtual day 6 and ending at 10:00am on virtual day 9. Furthermore, we considered a granularity of $4 \cdot 15$ minutes and $11 \cdot 60$ minutes, i.e., we have $n = 15$ timesteps and cover a time horizon of 12 hours. The cost parameters were set to $w^f f = 500.0$ for all $f \in \mathcal{F}$ and $w^a a = 5.0$ for all $a \in \mathcal{A}^{\text{ar}}$. For each simple state $s \in \mathcal{S}$ an individual cost $w^s \in \{0, \dots, 200\}$ for a change into it was fixed according to expert opinions.

Name	$ \mathcal{V}_i^{\text{fn}} $	$ \mathcal{V}_i^{\text{ar}} $	$ \mathcal{A}_i^{\text{ar}} $	$ \mathcal{A}_i^{\text{ar-pr}} $	$ \mathcal{F}_i $	$ \mathcal{S}_i $
A	2	0	3	2	3	5
B	2	0	4	3	2	5
C	6	1	10	1	4	4
D	3	0	5	3	6	10
E	6	0	9	2	12	13
F	6	2	12	3	3	14
G	10	2	24	5	18	32

Table 2: Overview of the properties of the 7 network stations A to G.

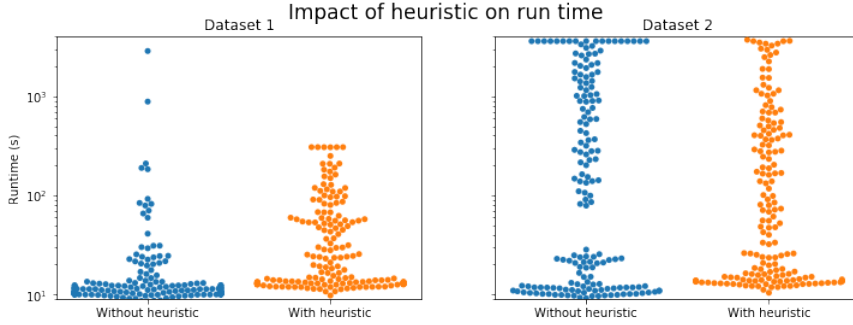


Figure 2: Runtimes of PURE (blue) and HEUR (orange). Each dot represents one instance, however dots may overlap when too many have similar run time. For the solution times, a logarithmic scale is used on the y-axis.

5.2 Computational Setup

We performed our computations on a cluster of machines composed of two *Intel Xeon Gold 5122* running at 3.60 GHz, which provide in total 8 cores and 96 GB of RAM. As solver for the underlying MILP problems we used *Gurobi* in version 8.1.0 [18], which was accessed via the native C interface. Since the corresponding MILP models turned out to be numerically challenging, we set the *NumericFocus* parameter to the maximum value and used the standard settings otherwise.

To each test instance we applied two versions of our solution approach. First, a pure approach, as it is described in the pseudocode (PURE) in Algorithm 1. And second, a version where both the RHH and the MCF heuristic were run before every MILP of the overall solving process (HEUR). In both cases, we set a cumulative timelimit of 3600 seconds for all MILPs. For HEUR, we additionally imposed a sub-timelimit of 300 seconds to each single MIP solve performed by RHH or MCF.

5.3 Results

Detailed computational results for all our testruns can be found in the table in Appendix A. First of all, for all but one instance, namely 6-0630, an optimal solution could be found by either the PURE or the HEUR approach. Additionally, for all but two instances feasible solutions without the usage of any slack could be found. For these two instances, namely 6-1530 and 7-2230, small amounts of boundary value slacks were needed at a single boundary node in one of the first two timesteps. A deeper analysis showed, that these small slacks were needed close to network stations, suggesting that a deeper investigation regarding the corresponding network stations is necessary. Interestingly, instance 6-1530 was solved much faster by PURE, even though the two heuristics found the optimal solution beforehand.

Next, we compare the performance of the PURE and the HEUR approach. The runtimes of the instances of the two data sets are plotted in Figure 2. As a first observation, both models were able to solve all instances within the time-limit. Additionally, the network seems to be somewhat stable w.r.t. to the necessary control decision considering the optimal solution values of first data set.

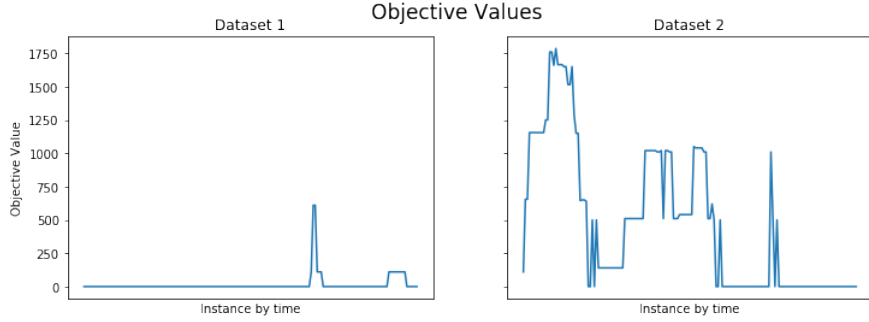


Figure 3: Objective values of the best found solutions for the instances ordered by time and linearly interpolated.

At a first glance PURE seems to outperform HEUR, although there are two instances, namely 3-2130 and 3-2200, where it needs 883 and 2863 seconds to solve in contrast to 173 and 155 seconds used by the HEUR approach, respectively. Interestingly, these are the two instances in the data set having the highest optimal solution value, i.e., the ones needing most control switches, see also Figure 3. However, a closer look on all results reveals, that most of the time used in the HEUR approach for instances with a runtime above 100 seconds was spent for the MCF heuristic, which does not seem to perform well here, as the results show. There are two exceptions, namely instances 3-2130 and 3-2200 again. Here, MCF seems to decrease the overall solution time by determining an optimal solution in 67 and 41 seconds, respectively.

For the second data set the analysis is a lot harder. First of all, there are 6 instances for which the PURE model fails to find a feasible solution, while HEUR is able to solve them to optimality. Additionally, besides the already mentioned instance 6-0630, there are 11 instances, which PURE could not solve within the timelimit. Overall, HEUR seems to have a slight advantage w.r.t. the running times and it is definitely more robust, as it always finds a feasible and except for two instances even an optimal one within the timelimit.

We did not expect that many jumps in the solution value curves in Figure 3, especially in data set 2. This is because the scenarios of two consecutive instances are closely connected and therefore we would expect constant objective values over longer time intervals. These abrupt changes suggest that a refinement of the network station model is necessary. For instances with high solution values in particular, we observed that flow direction changes happen very often between timesteps 0 and 1. This may indicate that the initially given flow values at the fence nodes call for a different flow direction than the one actually necessary for a stable network control. Thus, the mathematical formulation for the flow directions needs some improvement regarding noise in the data or the possible usage of the linepack in neighboring pipelines. Additionally, for network station D flow direction changes happened very often. Talking directly to dispatchers at OGE, this does not necessarily suggest an unstable behaviour and is actually very common. Hence, a refinement of the corresponding objective function parameter is necessary.

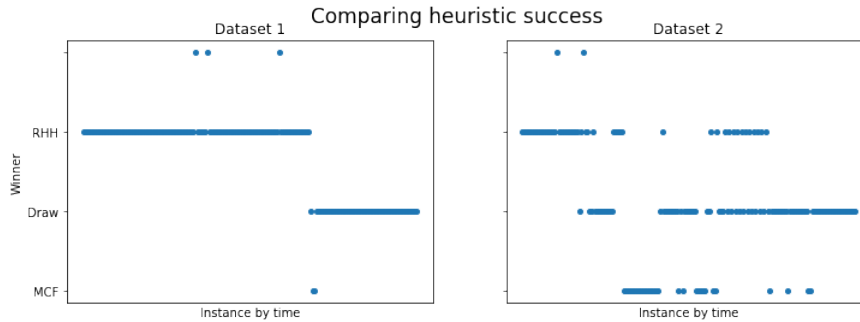


Figure 4: The dots represent the test instances, which are chronologically ordered on the x-axis. Each of them is assigned the value of that heuristic on the y-axis, which found a solution having smaller objective value. If both heuristics found solutions having the same objective value, its called a draw. The five dots on the top of the diagrams indicate instances for which only RHH found a feasible solution within the timelimit.

Finally, we compare the two heuristics within the HEUR approach. The plots in Figure 4 show which heuristic found a solution with smaller solution value. The five dots on the top show instances, for which MCF even failed to determine a feasible solution. Overall, RHH finds the better solution or at least draws with MCF and its runtime outperforms the runtime of MCF. Since MCF heavily relies on the concept of flow directions, this may be the reason for its weak performance. However, for some instances, for example instances 3-2130 and 3-2200 from data set 1 or instances 7-0030 to 07-0930 in data set 2, MCF finds better solutions. Since these are the ones with many control decisions to be taken, a further development of the heuristic seems to be a worthwhile idea

6 Conclusion and Outlook

In this paper we presented an optimization model for the control of transient gas transport networks. Here, complex pipeline intersection areas have been replaced by so-called network stations, i.e., by simplified hand-tailored graph representations modelling their technical capabilities. This formulation represents the first stage within a two stage approach for the NAVI, a decision support tool giving future non-technical and technical control recommendations for dispatchers. The goal of the model is to make important transient global control decisions, i.e., to determine the directions of the flow and where compression is necessary, which can later on be verified in a more detailed model described in [20]. Using a linearization of the Euler equations for the gas flow in pipelines and further approximations in particular regarding the compressor stations, we derive a trilevel MILP formulation, which can be solved using a sequence of (single-level) MILP formulations. For these MILPs, we developed heuristics, which determine initial solutions of good quality in rather short amounts of time and have a positive impact on the overall running times. Our computational experiments using actual historic flow and pressure values suggest that our model represents a valuable basis for further developments and extensions within the NAVI.

Regarding the model itself, the analysis of our computational results shows that a deeper investigation of the solutions w.r.t. the hand-tailored network stations has to follow. Further, an automated process to create these descriptions from the stations topology and the corresponding operations mode would improve the overall robustness and correctness of the approach. Another major point for further research is the currently used linearization of the Euler equations, where the absolute velocities in the friction term are fixed to a constant. While in many cases, when the gas flow on the pipelines is steady in speed over time, this does not affect the solution quality, it leads to problems in more vivid scenarios. Additionally, there is further potential for the modelling of the compressor arcs. Besides the obvious improvement of the approximation of the power bound, it would for example be nice to dynamically adapt the compression ratio in (41). Furthermore, it may be beneficial to increase the solving time by extending the model with a formulation for parallel and sequential setting choices to improve the overall quality of the solutions. From the application point of view, we currently aim at applying the model to larger parts of the network including more intersection areas. Finally, additional features like ramp-up times of compressor units and in general more detailed modelling approaches for the active elements could be added.

Acknowledgements

The work for this article has been conducted in the Research Campus MODAL funded by the German Federal Ministry of Education and Research (BMBF) (fund number 05M14ZAM).

References

- [1] Forschungscampus MODAL. <http://forschungscampus-modal.de/>. Accessed: 2019-10-31
- [2] Network data of Open Grid Europe GmbH. <https://www.open-grid-europe.com/cps/rde/oge-internet/hs.xsl/Strukturdaten-gemass-27-Abs-2-GasNEV-654.htm?rdeLocaleAttr=de>. Accessed: 2019-10-31
- [3] Open Grid Europe GmbH. <https://www.open-grid-europe.com/>. Accessed: 2019-10-31
- [4] Addis, B., Carello, G., Grosso, A., Tànfani, E.: Operating room scheduling and rescheduling: a rolling horizon approach. *Flexible Services and Manufacturing Journal* **28**(1-2), 206–232 (2016)
- [5] Alderson, D.L., Brown, G.G., Carlyle, W.M., Wood, R.K.: Solving Defender-Attacker-Defender Models for Infrastructure Defense. *Operations Research, Computing, and Homeland Defense, INFORMS* pp. 28–49 (2011)
- [6] Brotcorne, L., Labbé, M., Marcotte, P., Savard, G.: A bilevel model for toll optimization on a multicommodity transportation network. *Transportation science* **35**(4), 345–358 (2001)
- [7] Burlacu, R., Egger, H., Groß, M., Martin, A., Pfetsch, M., Schewe, L., Sirvent, M., Skutella, M.: Maximizing the storage capacity of gas networks: A global MINLP approach. *Optimization and Engineering* **20**(2), 543–573 (2019). DOI <https://doi.org/10.1007/s11081-018-9414-5>
- [8] Colson, B., Marcotte, P., Savard, G.: An overview of bilevel optimization. *Annals of operations research* **153**(1), 235–256 (2007)
- [9] Dell’Amico, M., Hadjidimitriou, N.S., Koch, T., Petkovic, M.: Forecasting natural gas flows in large networks. In: G. Nicosia, P. Pardalos, G. Giuffrida, R. Umeton (eds.) *Machine Learning, Optimization, and Big Data*, vol. 10710, pp. 158–171. Springer International Publishing, Cham (2018)
- [10] Dempe, S.: *Foundations of bilevel programming*. Springer Science & Business Media (2002)
- [11] Dempe, S., Kalashnikov, V., Ríos-Mercado, R.Z.: Discrete bilevel programming: Application to a natural gas cash-out problem. *European Journal of Operational Research* **166**(2), 469–488 (2005)
- [12] Federal Ministry for Economic Affairs and Energy: Still indispensable for a reliable energy supply. <https://www.bmwi.de/Redaktion/EN/Dossier/conventional-energy-sources.html> (2019). Accessed: 2019-10-31
- [13] Fügenschuh, A., Geißler, B., Gollmer, R., Morsi, A., Pfetsch, M.E., Rövekamp, J., Schmidt, M., Spreckelsen, K., Steinbach, M.C.: Physical and technical fundamentals of gas networks. In: Koch et al. [26]

- [14] Gao, Z., Wu, J., Sun, H.: Solution algorithm for the bi-level discrete network design problem. *Transportation Research Part B: Methodological* **39**(6), 479–495 (2005)
- [15] Garcia-Herreros, P., Zhang, L., Misra, P., Arslan, E., Mehta, S., Grossmann, I.E.: Mixed-integer bilevel optimization for capacity planning with rational markets. *Computers & Chemical Engineering* **86**, 33–47 (2016)
- [16] Grimm, V., Schewe, L., Schmidt, M., Zöttl, G.: A multilevel model of the European entry-exit gas market. *Mathematical Methods of Operations Research* **89**(2), 223–255 (2019)
- [17] Gugat, M., Leugering, G., Martin, A., Schmidt, M., Sirvent, M., Wintergerst, D.: MIP-based instantaneous control of mixed-integer PDE-constrained gas transport problems. *Computational Optimization and Applications* **70**(1), 267–294 (2018). DOI <https://doi.org/10.1007/s10589-017-9970-1>
- [18] Gurobi Optimization, L.: Gurobi optimizer reference manual, version 8.1.0. <http://www.gurobi.com> (2018)
- [19] Hennings, F.: Benefits and Limitations of Simplified Transient Gas Flow Formulations. In: *Operations Research Proceedings 2017*, pp. 231–237. Springer (2018)
- [20] Hennings, F., Anderson, L., Hoppmann, K., Turner, M., Koch, T.: Controlling transient gas flow in real-world pipeline intersection areas. Tech. Rep. 19-24, ZIB, Takustr. 7, 14195 Berlin (2019)
- [21] Hoppmann, K., Schwarz, R.: Finding maximum minimum cost flows to evaluate gas network capacities. In: *Operations Research Proceedings 2017*, pp. 339 – 346 (2018)
- [22] Jiang, R., Wang, J., Guan, Y.: Robust Unit Commitment With Wind Power and Pumped Storage Hydro. *IEEE Transactions on Power Systems* **27**(2), 800–810 (2011)
- [23] Kalashnikov, V.V., Dempe, S., Pérez-Valdés, G.A., Kalashnykova, N.I., Camacho-Vallejo, J.F.: Bilevel Programming and Applications. *Mathematical Problems in Engineering* **2015** (2015)
- [24] Kalashnikov, V.V., Ríos-Mercado, R.Z.: Solving a natural gas cash-out bilevel program by a penalty function method. Tech. Rep. PISIS-2002-03, Graduate Program in Systems Engineering, UANL, San Nicolás de los Garza, México (2002)
- [25] Koch, T., Chen, Y., Gamrath, I., Gotzes, U., Petkovic, M., Hadjidimitriou, N.S., Zittel, J.: High precision prediction of gas flows. Tech. Rep. 19-26, ZIB, Takustr. 7, 14195 Berlin (2019)
- [26] Koch, T., Hiller, B., Pfetsch, M.E., Schewe, L. (eds.): Evaluating Gas Network Capacities, *MOS-SIAM Series on Optimization*, vol. 21. SIAM (2015)
- [27] Lu, J., Han, J., Hu, Y., Zhang, G.: Multilevel decision-making: A survey. *Information Sciences* **346**, 463–487 (2016)

- [28] Mak, T.W., Van Hentenryck, P., Zlotnik, A., Hijazi, H., Bent, R.: Efficient dynamic compressor optimization in natural gas transmission systems. In: American Control Conference (ACC), 2016, pp. 7484–7491. IEEE (2016). DOI <https://doi.org/10.1109/ACC.2016.7526855>
- [29] Migdalas, A., Pardalos, P.M., Värbrand, P.: Multilevel Optimization: Algorithms and Applications, vol. 20. Springer Science & Business Media (2013)
- [30] Moritz, S.: A mixed integer approach for the transient case of gas network optimization. Ph.D. thesis, Technische Universität Darmstadt, Darmstadt (2007)
- [31] Nielsen, L.K., Kroon, L., Maróti, G.: A rolling horizon approach for disruption management of railway rolling stock. *European Journal of Operational Research* **220**(2), 496–509 (2012)
- [32] Nikuradse, J.: *Laws of Flow in Rough Pipes*. National Advisory Committee for Aeronautics Washington (1950)
- [33] Osiadacz, A.J.: Different Transient Flow Models - Limitations, Advantages, And Disadvantages. In: PSIG-9606. Pipeline Simulation Interest Group (1996)
- [34] Rövekamp, J.: Background on gas market regulation. In: Koch et al. [26]
- [35] Saleh, J.M.: *Fluid Flow Handbook*. McGraw-Hill Professional (2002)
- [36] Samà, M., D’Ariano, A., Pacciarelli, D.: Rolling Horizon Approach for Aircraft Scheduling in the Terminal Control Area of Busy Airports. *Procedia-Social and Behavioral Sciences* **80**, 531–552 (2013)
- [37] Steringa, J.J., Hoogwerf, M., Dijkhuis, H., et al.: A Systematic Approach to Transmission Stress Tests in Entry-Exit Systems. In: PSIG Annual Meeting. Pipeline Simulation Interest Group (2015)
- [38] Wayne Winegarden: Low- and no-carbon future starts with natural gas. <https://www.washingtonpost.com/brand-studio/wp/2019/02/15/low-and-no-carbon-future-starts-with-natural-gas/> (2019). Accessed: 2019-10-31
- [39] Zlotnik, A., Chertkov, M., Backhaus, S.: Optimal control of transient flow in natural gas networks. In: 54th IEEE Conference on Decision and Control (CDC), pp. 4563–4570. IEEE (2015). DOI <https://doi.org/10.1109/CDC.2015.7402932>

A Appendix

The columns of the following tables contain the results of the computational experiments discussed in Section 5. In the following, the solution values here are stated w.r.t. the objective function of the third level (53), i.e., the cost of the slacks is excluded. The 1st column contains the name of the instance. They consist of the virtual day together with the time in hours and minutes of corresponding initial state, i.e., 2-0400 is the instance having the initial state from virtual day 2 at 4am. The 2nd column denotes the runtime of the PURE solution algorithm. The 3rd and 4th column show the value of the best solution found and the final MILP gap. In case these columns contain a hyphen, the approach did not find a feasible solution within the timelimit. The 5th, 6th and 7th column contain the corresponding entities for the HEUR approach. Furthermore, the 8th and the 9th as well as the 10th and the 11th column display the accumulated runtimes and values of the solution obtained by the RHH and the MCF heuristics, respectively. Again, a hyphen indicates that no solution was found within the timelimit. For the two underlined instances, flow slack had to be used to derive a feasible solution.

Inst	PURE	Val	Gap	HEUR	Val	Gap	RHH	Val	MCF	Val
1-1200	10.6	0	0	11.9	0	0	5.0	0	6.9	605
1-1230	9.0	0	0	10.7	0	0	4.9	0	5.8	605
1-1300	10.4	0	0	11.5	0	0	5.1	0	6.4	605
1-1330	10.3	0	0	10.7	0	0	4.6	0	6.1	605
1-1400	15.5	0	0	11.8	0	0	4.5	0	7.3	605
1-1430	10.1	0	0	12.5	0	0	5.2	0	7.2	605
1-1500	10.8	0	0	11.8	0	0	4.9	0	6.9	605
1-1530	9.9	0	0	13.0	0	0	5.1	0	7.9	605
1-1600	13.0	0	0	13.0	0	0	5.5	0	7.6	605
1-1630	10.8	0	0	11.3	0	0	5.2	0	6.1	605
1-1700	10.7	0	0	12.8	0	0	5.3	0	7.4	605
1-1730	10.1	0	0	11.9	0	0	5.3	0	6.6	605
1-1800	9.5	0	0	11.9	0	0	5.3	0	6.7	605
1-1830	10.1	0	0	11.8	0	0	4.8	0	7.1	605
1-1900	21.5	0	0	12.6	0	0	5.3	0	7.3	605
1-1930	9.9	0	0	11.8	0	0	5.2	0	6.6	605
1-2000	11.3	0	0	12.5	0	0	4.9	0	7.6	605
1-2030	11.9	0	0	9.7	0	0	4.8	0	4.9	605
1-2100	10.6	0	0	13.1	0	0	4.7	0	8.4	605
1-2130	10.0	0	0	11.6	0	0	5.3	0	6.3	605
1-2200	12.3	0	0	11.3	0	0	5.4	0	5.9	605
1-2230	9.5	0	0	11.5	0	0	5.5	0	6.0	605
1-2300	9.7	0	0	14.0	0	0	5.3	0	8.7	605
1-2330	10.1	0	0	12.7	0	0	5.3	0	7.4	605
2-0000	11.0	0	0	12.5	0	0	5.2	0	7.2	605
2-0030	13.0	0	0	12.0	0	0	5.2	0	6.9	605
2-0100	10.6	0	0	12.9	0	0	5.5	0	7.4	605
2-0130	10.6	0	0	11.8	0	0	4.8	0	7.0	605
2-0200	11.3	0	0	12.8	0	0	5.1	0	7.7	605
2-0230	10.6	0	0	12.7	0	0	5.4	0	7.3	605
2-0300	10.5	0	0	19.2	0	0	5.0	0	14.2	605
2-0330	10.7	0	0	13.0	0	0	5.4	0	7.6	605
2-0400	13.4	0	0	12.9	0	0	4.8	0	8.0	605
2-0430	10.0	0	0	18.8	0	0	5.2	0	13.5	605
2-0500	24.5	0	0	12.6	0	0	5.0	0	7.6	605
2-0530	11.4	0	0	12.5	0	0	5.4	0	7.2	605
2-0600	10.3	0	0	12.0	0	0	5.2	0	6.7	605
2-0630	16.0	0	0	11.2	0	0	4.7	0	6.5	605
2-0700	9.9	0	0	11.9	0	0	5.2	0	6.7	605
2-0730	10.1	0	0	13.2	0	0	5.3	0	7.9	605
2-0800	10.9	0	0	16.4	0	0	5.3	0	11.1	605
2-0830	9.4	0	0	12.6	0	0	4.8	0	7.8	605
2-0900	9.7	0	0	12.3	0	0	5.3	0	7.0	605

Inst	PURE	Val	Gap	HEUR	Val	Gap	RHH	Val	MCF	Val
2-0930	10.6	0	0	13.1	0	0	5.3	0	7.7	605
2-1000	10.0	0	0	13.1	0	0	5.3	0	7.7	605
2-1030	20.7	0	0	12.2	0	0	5.6	0	6.7	605
2-1100	12.2	0	0	13.3	0	0	5.3	0	8.0	605
2-1130	12.6	0	0	29.9	0	0	5.4	0	24.5	1245
2-1200	9.9	0	0	118.4	0	0	5.4	0	113.1	1245
2-1230	13.3	0	0	83.7	0	0	5.5	0	78.2	1245
2-1300	10.0	0	0	208.2	0	0	5.3	0	202.9	1245
2-1330	13.7	0	0	249.5	0	0	5.7	0	243.8	1245
2-1400	11.0	0	0	305.3	0	0	5.3	0	300.0	1245
2-1430	12.3	0	0	208.0	0	0	5.5	0	202.5	1245
2-1500	10.0	0	0	306.1	0	0	6.1	0	300.0	1245
2-1530	9.8	0	0	149.0	0	0	5.6	0	143.3	1245
2-1600	10.0	0	0	305.8	0	0	5.8	0	300.0	-
2-1630	9.9	0	0	23.4	0	0	6.2	0	17.3	1245
2-1700	10.8	0	0	96.9	0	0	5.7	0	91.2	1245
2-1730	9.0	0	0	306.2	0	0	6.1	0	300.0	1250
2-1800	13.7	0	0	86.0	0	0	5.9	0	80.1	1245
2-1830	10.7	0	0	190.4	0	0	5.1	0	185.3	1245
2-1900	8.6	0	0	305.7	0	0	5.7	0	300.0	-
2-1930	10.0	0	0	62.0	0	0	5.5	0	56.5	1245
2-2000	8.7	0	0	67.6	0	0	5.6	0	62.0	1245
2-2030	10.1	0	0	82.2	0	0	5.4	0	76.8	1245
2-2100	10.1	0	0	54.3	0	0	5.4	0	48.9	1245
2-2130	10.0	0	0	12.8	0	0	5.5	0	7.3	1245
2-2200	9.9	0	0	95.6	0	0	5.6	0	90.0	1245
2-2230	9.8	0	0	55.3	0	0	6.0	0	49.2	635
2-2300	10.0	0	0	48.8	0	0	5.8	0	43.0	635
2-2330	14.6	0	0	110.8	0	0	5.5	0	105.3	635
3-0000	11.5	0	0	79.8	0	0	5.1	0	74.7	635
3-0030	12.1	0	0	57.8	0	0	5.1	0	52.7	635
3-0100	11.6	0	0	57.2	0	0	5.7	0	51.5	635
3-0130	14.6	0	0	24.4	0	0	4.9	0	19.5	635
3-0200	10.0	0	0	99.6	0	0	5.8	0	93.8	635
3-0230	12.8	0	0	55.9	0	0	5.6	0	50.3	635
3-0300	10.6	0	0	114.8	0	0	4.8	0	110.0	635
3-0330	11.0	0	0	53.2	0	0	5.1	0	48.1	635
3-0400	12.2	0	0	14.5	0	0	5.7	0	8.8	635
3-0430	11.4	0	0	59.4	0	0	4.9	0	54.5	635
3-0500	8.6	0	0	51.9	0	0	4.8	0	47.1	635
3-0530	11.8	0	0	47.4	0	0	5.5	0	41.9	635
3-0600	12.7	0	0	67.2	0	0	5.3	0	61.9	635
3-0630	17.5	0	0	36.3	0	0	5.7	0	30.5	635
3-0700	10.1	0	0	40.5	0	0	5.2	0	35.3	1245
3-0730	20.4	0	0	20.9	0	0	5.8	0	15.2	1245
3-0800	11.5	0	0	90.5	0	0	5.8	0	84.8	1245
3-0830	11.6	0	0	90.0	0	0	5.8	0	84.2	1245
3-0900	11.0	0	0	14.2	0	0	5.5	0	8.6	1245
3-0930	11.5	0	0	50.9	0	0	5.9	0	45.0	1245
3-1000	12.2	0	0	25.1	0	0	5.7	0	19.4	1245
3-1030	10.1	0	0	97.9	0	0	5.4	0	92.5	1245
3-1100	10.8	0	0	55.4	0	0	6.1	0	49.4	1245
3-1130	9.7	0	0	11.9	0	0	4.4	0	7.5	1245
3-1200	11.8	0	0	57.3	0	0	5.4	0	51.9	1245
3-1230	10.9	0	0	44.7	0	0	6.7	0	38.0	1245
3-1300	22.4	0	0	300.3	0	0	6.2	0	300.0	-
3-1330	23.6	0	0	181.5	0	0	5.5	0	175.9	1245
3-1400	11.4	0	0	161.9	0	0	5.3	0	156.6	1245
3-1430	22.7	0	0	209.0	0	0	5.5	0	203.5	1245
3-1500	11.4	0	0	109.1	0	0	5.6	0	103.6	1245
3-1530	9.1	0	0	129.4	0	0	5.0	0	124.3	1245

Inst	PURE	Val	Gap	HEUR	Val	Gap	RHH	Val	MCF	Val
3-1600	10.5	0	0	127.4	0	0	4.4	0	122.9	1245
3-1630	11.8	0	0	118.8	0	0	5.5	0	113.2	1245
3-1700	9.6	0	0	109.0	0	0	5.2	0	103.7	1245
3-1730	59.4	0	0	13.5	0	0	5.3	0	8.2	605
3-1800	31.0	0	0	13.9	0	0	5.4	0	8.5	605
3-1830	10.1	0	0	19.2	0	0	5.3	0	13.9	605
3-1900	10.2	0	0	50.5	0	0	5.0	0	45.4	605
3-1930	30.0	0	0	13.3	0	0	5.4	0	7.9	605
3-2000	10.0	0	0	32.6	0	0	5.1	0	27.5	605
3-2030	12.2	0	0	18.2	0	0	4.9	0	13.4	605
3-2100	70.1	110	0	27.8	110	0	7.3	110	14.2	110
3-2130	882.9	610	0	173.4	610	0	8.6	736	67.4	610
3-2200	2 862.9	610	0	155.1	610	0	9.1	736	41.6	610
3-2230	10.2	110	0	17.6	110	0	8.0	110	8.1	110
3-2300	65.5	110	0	16.7	110	0	7.7	110	7.8	110
3-2330	78.8	110	0	58.9	110	0	9.4	110	48.3	110
4-0000	30.9	0	0	13.5	0	0	5.2	0	8.3	0
4-0030	20.1	0	0	22.9	0	0	5.1	0	17.9	0
4-0100	10.6	0	0	53.2	0	0	5.4	0	47.8	0
4-0130	11.1	0	0	25.5	0	0	6.0	0	19.5	0
4-0200	19.5	0	0	13.4	0	0	4.8	0	8.6	0
4-0230	10.6	0	0	13.2	0	0	5.3	0	7.9	0
4-0300	23.9	0	0	13.3	0	0	5.4	0	7.9	0
4-0330	11.5	0	0	12.7	0	0	4.7	0	8.0	0
4-0400	10.6	0	0	13.2	0	0	4.8	0	8.4	0
4-0430	10.7	0	0	13.4	0	0	4.8	0	8.5	0
4-0500	10.6	0	0	14.6	0	0	5.1	0	9.5	0
4-0530	9.3	0	0	14.9	0	0	4.9	0	10.0	0
4-0600	11.3	0	0	14.7	0	0	5.4	0	9.3	0
4-0630	8.5	0	0	13.3	0	0	5.2	0	8.1	0
4-0700	9.7	0	0	12.9	0	0	5.1	0	7.8	0
4-0730	16.9	0	0	13.9	0	0	4.6	0	9.3	0
4-0800	10.8	0	0	12.9	0	0	5.1	0	7.8	0
4-0830	11.2	0	0	12.7	0	0	5.3	0	7.5	0
4-0900	12.5	0	0	14.2	0	0	5.0	0	9.3	0
4-0930	13.4	0	0	23.4	0	0	4.6	0	18.8	0
4-1000	12.9	0	0	16.4	0	0	4.9	0	11.5	0
4-1030	11.9	0	0	12.7	0	0	4.7	0	8.0	0
4-1100	12.9	0	0	13.2	0	0	5.1	0	8.1	0
4-1130	29.2	0	0	19.8	0	0	5.3	0	14.5	0
4-1200	12.3	0	0	13.6	0	0	5.0	0	8.6	0
4-1230	24.3	0	0	12.9	0	0	5.0	0	7.9	0
4-1300	11.5	0	0	14.8	0	0	5.7	0	9.1	0
4-1330	10.3	0	0	12.6	0	0	5.0	0	7.6	0
4-1400	10.6	0	0	14.4	0	0	5.1	0	9.3	0
4-1430	12.4	0	0	13.9	0	0	5.6	0	8.2	0
4-1500	11.3	0	0	24.1	0	0	5.0	0	7.7	0
4-1530	11.0	0	0	36.8	0	0	5.7	0	20.0	0
4-1600	10.4	0	0	23.8	0	0	5.6	0	7.9	0
4-1630	188.8	110	0	29.7	110	0	7.7	110	17.0	110
4-1700	81.8	110	0	67.2	110	0	7.7	110	53.1	110
4-1730	209.5	110	0	53.5	110	0	7.6	110	39.7	110
4-1800	21.6	110	0	42.9	110	0	7.5	110	34.2	110
4-1830	183.2	110	0	29.5	110	0	7.4	110	15.6	110
4-1900	92.0	110	0	31.3	110	0	7.6	110	16.9	110
4-1930	83.6	110	0	28.4	110	0	7.1	110	20.0	110
4-2000	40.9	110	0	46.4	110	0	7.8	110	37.2	110
4-2030	25.3	110	0	44.4	110	0	7.4	110	35.8	110
4-2100	12.3	0	0	12.7	0	0	5.5	0	7.2	0
4-2130	12.3	0	0	15.4	0	0	5.6	0	9.8	0
4-2200	11.6	0	0	13.0	0	0	4.6	0	8.4	0
4-2230	12.1	0	0	13.5	0	0	5.7	0	7.9	0
4-2300	11.3	0	0	13.8	0	0	5.0	0	8.9	0
4-2330	11.3	0	0	24.0	0	0	5.0	0	7.8	0

Inst	PURE	Val	Gap	HEUR	Val	Gap	RHH	Val	MCF	Val
6-0000	897.1	110	0	166.4	110	0	12.9	115	52.7	500
6-0030	1 514.7	655	0	683.3	655	0	11.3	765	56.4	1010
6-0100	3 218.0	655	0	319.1	655	0	13.1	765	69.5	1010
6-0130	1 009.8	1155	0	506.6	1155	0	13.0	1265	37.6	1510
6-0200	895.4	1155	0	1 060.2	1155	0	13.5	1260	40.4	1510
6-0230	3 600.0	1155	0.11	896.4	1155	0	11.3	1260	64.3	1510
6-0300	1 758.2	1155	0	418.2	1155	0	11.9	1260	42.8	1510
6-0330	3 600.0	1155	0.087	1 149.5	1155	0	12.1	1260	41.1	2190
6-0400	1 410.0	1155	0	732.4	1155	0	11.1	1260	7.6	2190
6-0430	1 652.9	1155	0	1 217.2	1155	0	12.4	1260	300.0	2335
6-0500	3 600.0	1275	0.21	812.5	1155	0	12.1	1260	300.0	2345
6-0530	3 600.0	2161	0.522	457.6	1250	0	18.0	1260	300.0	4010
6-0600	1 926.9	1250	0	403.9	1250	0	16.9	1260	300.0	4560
6-0630	3 600.0	1760	0.13	3 600.0	1760	0.134	13.1	1770	165.9	3330
6-0700	3 600.0	-	-	3 397.3	1760	0	12.9	1770	291.4	3330
6-0730	3 600.0	-	-	2 610.2	1660	0	12.5	1770	300.0	2970
6-0800	258.4	1786	0	324.0	1786	0	12.6	1786	300.0	3485
6-0830	3 600.0	2910	0.478	1 059.8	1665	0	13.0	1775	300.0	-
6-0900	3 600.0	1770	0.146	2 247.1	1665	0	12.9	1775	300.0	3330
6-0930	1 754.6	1665	0	570.2	1665	0	12.8	1775	300.0	3330
6-1000	2 347.1	1650	0	3 487.2	1650	0	12.3	1775	245.3	2955
6-1030	2 667.7	1650	0	361.8	1650	0	12.8	1665	300.0	3455
6-1100	1 051.9	1515	0	535.1	1515	0	12.2	1770	161.8	2820
6-1130	1 353.9	1515	0	453.1	1515	0	8.8	1880	64.9	2820
6-1200	2 076.0	1650	0	408.3	1650	0	8.5	1930	109.7	2955
6-1230	3 600.0	-	-	399.3	1290	0	18.6	1935	137.3	2610
6-1300	2 169.0	1150	0	366.5	1150	0	18.2	1655	103.6	2470
6-1330	3 600.0	-	-	548.1	1150	0	18.0	1795	162.6	2470
6-1400	548.4	645	0	374.1	645	0	15.9	645	300.0	645
6-1430	584.8	650	0	232.5	650	0	16.1	650	161.1	1970
6-1500	3 600.0	-	-	597.0	650	0	16.3	650	300.0	-
6-1530	880.1	640	0	2 763.5	640.0	0	29.8	640	89.9	640
6-1600	85.4	0	0	79.1	0	0	6.1	500	44.5	1305
6-1630	106.1	0	0	71.6	0	0	8.8	0	62.8	0
6-1700	9.9	500	0	90.8	500	0	6.7	500	81.3	500
6-1730	163.0	0	0	13.5	0	0	6.3	0	7.3	1000
6-1800	9.1	500	0	116.7	500	0	5.7	500	109.6	500
6-1830	10.4	140	0	61.0	140	0	8.5	140	51.5	140
6-1900	11.1	140	0	84.5	140	0	8.6	140	74.9	140
6-1930	15.0	140	0	16.8	140	0	8.0	140	7.8	140
6-2000	109.7	140	0	25.1	140	0	8.1	140	12.6	140
6-2030	133.7	140	0	16.9	140	0	7.8	140	8.2	140
6-2100	14.9	140	0	80.4	140	0	8.4	140	71.0	140
6-2130	81.7	140	0	23.5	140	0	8.6	140	13.9	140
6-2200	214.8	140	0	55.7	140	0	7.8	140	46.9	140
6-2230	138.0	140	0	42.3	140	0	7.9	140	33.4	640
6-2300	201.2	140	0	68.1	140	0	8.1	140	58.9	640
6-2330	141.9	140	0	15.6	140	0	7.7	140	6.9	640
7-0000	147.3	140	0	15.0	140	0	7.7	140	6.3	640
7-0030	28.3	140	0	19.6	140	0	9.0	140	9.5	640
7-0100	1 005.4	510	0	1 017.2	510	0	9.5	650	8.9	510
7-0130	226.9	510	0	187.4	510	0	7.9	650	10.9	510
7-0200	424.2	510	0	138.5	510	0	11.9	650	27.8	510
7-0230	447.7	510	0	55.3	510	0	9.9	650	8.2	510
7-0300	523.5	510	0	160.7	510	0	11.8	650	70.4	510
7-0330	281.4	510	0	3273.2	510	0	10.4	650	15.3	510
7-0400	316.2	510	0	168.1	510	0	10.5	650	9.6	510
7-0430	272.6	510	0	165.3	510	0	10.6	650	57.1	510
7-0500	367.7	510	0	132.0	510	0	10.8	650	8.0	510
7-0530	1 026.8	510	0	48.2	510	0	11.0	650	11.0	510
7-0600	1 563.6	1020	0	1 879.8	1020	0	13.0	1160	94.5	1020
7-0630	2 580.5	1020	0	1 543.0	1020	0	15.1	1160	181.5	1020
7-0700	1 152.5	1020	0	701.2	1020	0	17.0	1160	125.7	1020

Inst	PURE	Val	Gap	HEUR	Val	Gap	RHH	Val	MCF	Val
7-0730	2 691.0	1020	0	1 305.0	1020	0	16.6	1160	143.8	1020
7-0800	2 027.3	1020	0	684.1	1020	0	17.8	1160	25.5	1020
7-0830	1 652.8	1020	0	1 148.3	1020	0	18.5	1160	70.0	1020
7-0900	3 600.0	1030	0.511	282.2	1010	0	14.1	1150	76.2	1010
7-0930	1 427.5	1010	0	3 600.0	1010	0	12.8	1150	38.6	1010
7-1000	3 600.0	1020	0.195	2 483.1	1020	0	13.9	1020	88.8	1020
7-1030	340.6	510	0	203.4	510	0	12.9	510	45.9	1010
7-1100	745.3	1020	0	245.0	1020	0	20.6	1020	85.5	1020
7-1130	3 600.0	1020	0.009	775.4	1020	0	21.8	1020	101.1	1020
7-1200	2 163.7	1010	0	3 025.8	1010	0	13.1	1010	64.5	1010
7-1230	690.4	1010	0	495.2	1010	0	8.2	1010	8.8	1010
7-1300	12.7	510	0	33.3	510	0	12.0	510	9.6	510
7-1330	762.2	510	0	70.6	510	0	11.1	510	10.5	510
7-1400	11.7	510	0	98.3	510	0	14.2	510	75.2	510
7-1430	3 341.2	540	0	3 392.8	540	0	64.4	680	252.3	540
7-1500	905.8	540	0	402.9	540	0	99.8	540	279.5	540
7-1530	1 238.2	540	0	1 888.4	540	0	53.4	680	173.7	540
7-1600	360.5	540	0	278.3	540	0	99.0	540	150.3	540
7-1630	3 081.0	540	0	3 245.4	540	0	86.1	540	157.9	540
7-1700	1 223.9	540	0	274.8	540	0	94.4	540	153.0	540
7-1730	3 600.0	540	0.054	3 600.0	540	0	88.0	540	256.4	540
7-1800	3 600.0	-	-	1 532.4	1050	0	92.4	1050	186.9	1050
7-1830	2 886.5	1040	0	2 944.5	1040	0	74.5	1040	233.8	1040
7-1900	3 600.0	1170	0.132	290.0	1040	0	67.4	1190	173.9	1040
7-1930	2 707.1	1040	0	3 600.0	1040	0.018	56.2	1190	214.5	1040
7-2000	278.9	1040	0	478.0	1040	0	125.5	1150	300.0	1080
7-2030	287.5	1010	0	138.4	1010	0	11.2	1120	13.2	1010
7-2100	231.6	1010	0	271.2	1010	0	19.2	1020	63.6	1010
7-2130	153.1	510	0	47.5	510	0	13.7	510	13.8	510
7-2200	139.0	510	0	100.5	510	0	13.8	510	68.5	510
7-2230	617.7	620	0	172.9	620	0	39.0	620	91.3	640
7-2300	90.5	500	0	16.0	500	0	8.0	610	6.9	500
7-2330	10.3	0	0	13.7	0	0	5.9	500	7.8	0
8-0000	9.7	0	0	13.9	0	0	6.3	0	7.6	1000
8-0030	99.1	500	0	14.5	500	0	7.5	500	6.0	500
8-0100	9.9	0	0	11.8	0	0	5.2	0	6.5	0
8-0130	11.7	0	0	12.1	0	0	5.9	0	6.2	0
8-0200	10.4	0	0	12.0	0	0	5.4	0	6.6	500
8-0230	10.1	0	0	10.4	0	0	4.7	0	5.6	0
8-0300	11.5	0	0	18.4	0	0	8.0	0	10.4	1000
8-0330	9.8	0	0	13.5	0	0	7.3	0	6.1	0
8-0400	10.9	0	0	12.1	0	0	5.5	0	6.6	1000
8-0430	10.5	0	0	12.7	0	0	6.4	0	6.3	0
8-0500	9.6	0	0	12.7	0	0	5.4	0	7.3	1000
8-0530	9.6	0	0	13.1	0	0	5.5	0	7.6	0
8-0600	10.6	0	0	12.3	0	0	5.2	0	7.1	1000
8-0630	9.2	0	0	13.1	0	0	6.0	0	7.1	0
8-0700	21.3	0	0	18.0	0	0	6.4	140	7.1	1000
8-0730	10.1	0	0	12.1	0	0	5.8	0	6.3	0
8-0800	10.7	0	0	14.1	0	0	5.8	0	8.3	1000
8-0830	10.1	0	0	13.6	0	0	6.2	0	7.4	0
8-0900	10.1	0	0	14.1	0	0	5.4	0	8.7	1000
8-0930	11.6	0	0	13.2	0	0	4.8	0	8.4	0
8-1000	13.3	0	0	25.5	0	0	7.4	140	9.8	1000
8-1030	10.2	0	0	12.5	0	0	5.2	0	7.3	0
8-1100	12.0	0	0	33 20.7	0	0	6.9	140	8.2	1000
8-1130	10.0	0	0	12.8	0	0	5.1	0	7.8	0
8-1200	18.9	0	0	12.6	0	0	5.3	0	7.4	1000

Inst	PURE	Val	Gap	HEUR	Val	Gap	RHH	Val	MCF	Val
8-1230	10.3	0	0	13.6	0	0	5.2	0	8.4	0
8-1300	588.9	1010	0	191.5	1010	0	8.4	1150	44.4	1010
8-1330	78.6	510	0	47.1	510	0	14.2	510	10.5	510
8-1400	12.0	0	0	13.4	0	0	5.3	0	8.1	0
8-1430	12.6	500	0	17.9	500	0	7.1	500	7.9	500
8-1500	11.7	0	0	16.1	0	0	4.9	0	11.2	0
8-1530	22.8	0	0	17.5	0	0	5.4	0	12.2	0
8-1600	21.1	0	0	15.0	0	0	5.6	0	9.4	0
8-1630	23.7	0	0	52.2	0	0	6.0	0	46.2	0
8-1700	25.4	0	0	13.9	0	0	5.5	0	8.4	0
8-1730	21.8	0	0	15.6	0	0	7.8	140	7.8	0
8-1800	24.7	0	0	14.7	0	0	5.8	0	8.9	0
8-1830	22.6	0	0	13.4	0	0	5.5	0	7.9	0
8-1900	11.7	0	0	20.2	0	0	4.8	0	15.5	0
8-1930	11.3	0	0	11.8	0	0	4.8	0	7.0	0
8-2000	9.9	0	0	11.1	0	0	5.1	0	6.0	0
8-2030	20.9	0	0	14.3	0	0	5.3	0	9.0	0
8-2100	23.1	0	0	13.6	0	0	6.2	0	7.4	0
8-2130	16.4	0	0	23.4	0	0	6.0	0	17.4	0
8-2200	22.2	0	0	12.7	0	0	5.1	0	7.6	0
8-2230	22.3	0	0	25.8	0	0	7.6	140	18.2	0
8-2300	24.1	0	0	39.9	0	0	6.3	0	33.5	0
8-2330	13.1	0	0	16.3	0	0	5.5	0	10.8	0
9-0000	11.1	0	0	12.9	0	0	6.1	0	6.8	0
9-0030	12.2	0	0	24.6	0	0	5.4	0	7.0	0
9-0100	9.8	0	0	13.2	0	0	6.1	0	7.0	0
9-0130	11.1	0	0	23.8	0	0	4.8	0	7.8	0
9-0200	11.7	0	0	13.2	0	0	5.3	0	7.9	0
9-0230	12.1	0	0	25.8	0	0	6.3	0	7.4	0
9-0300	10.8	0	0	13.7	0	0	6.9	0	6.8	0
9-0330	11.4	0	0	13.8	0	0	6.9	0	6.9	0
9-0400	12.7	0	0	26.0	0	0	6.4	0	7.0	0
9-0430	11.5	0	0	12.9	0	0	5.7	0	7.3	0
9-0500	9.7	0	0	12.8	0	0	5.9	0	6.9	0
9-0530	10.9	0	0	14.7	0	0	7.9	0	6.8	0
9-0600	18.5	0	0	16.0	0	0	9.3	0	6.7	0
9-0630	11.8	0	0	15.2	0	0	6.9	0	8.3	0
9-0700	11.7	0	0	13.8	0	0	5.5	0	8.2	0
9-0730	23.9	0	0	14.8	0	0	7.2	0	7.6	0
9-0800	20.6	0	0	33.2	0	0	5.9	0	6.8	0
9-0830	10.9	0	0	13.0	0	0	6.0	0	6.9	0
9-0900	18.7	0	0	32.0	0	0	5.7	0	7.7	0
9-0930	10.8	0	0	12.2	0	0	4.6	0	7.6	0
9-1000	20.7	0	0	13.7	0	0	6.2	0	7.5	0